

CROSSED HOT-WIRE MEASUREMENTS IN LOW REYNOLDS
NUMBER SUPERSONIC JETS

By

JERRY DALE SWEARINGEN

Bachelor of Science in Mechanical Engineering

Oklahoma State University

Stillwater, Oklahoma

1977

Submitted to the Faculty of the Graduate College
of the Oklahoma State University
in partial fulfillment of the requirements
for the Degree of
MASTER OF SCIENCE
December, 1979

Thesis
1979
5974c
cop.2



CROSSED HOT-WIRE MEASUREMENTS IN LOW REYNOLDS
NUMBER SUPERSONIC JETS

Thesis Approved:

Dennis K. McLaughlin

Thesis Adviser

R. F. Lowery

David G. Rillee

Norman N. Rumban

Dean of the Graduate College

1043075

ACKNOWLEDGMENTS

The author wishes to express his appreciation to his major adviser, Dr. Dennis K. McLaughlin, and to his other committee members, Dr. David G. Lilley and Dr. Richard L. Lowery, for their advice and guidance concerning this work. Appreciation is also expressed to Dr. Tim R. Troutt for his assistance with the experiments and helpful comments on the work. The author would also like to express his gratitude to Charlene Fries for the final typing of the text.

The author also recognizes the financial support of the National Aeronautics and Space Administration through Grant No. NSG 1467.

TABLE OF CONTENTS

Chapter	Page
I. INTRODUCTION	1
A. Background	1
B. Subject of Research	2
C. Objectives	4
II. EXPERIMENTAL APPARATUS	6
A. General Facility	6
B. Instrumentation	8
III. EXPERIMENTAL PROCEDURES	11
A. General	11
B. Crossed Hot-Wire Procedure and Data Analysis	11
C. Phase-Averaging Procedure	16
IV. EXPERIMENTAL RESULTS	18
A. Crossed Hot-Wire Measurements	18
B. Phase-Average Measurements	27
V. CONCLUSIONS	30
A. Summary	30
B. Recommendations for Further Study	31
BIBLIOGRAPHY	34
APPENDIX - FIGURES	37

LIST OF FIGURES

Figure	Page
1. Schematic of Overall Facility	38
2. Schematic of Test Chamber	39
3. Crossed Hot-Wire Probe, Full Scale	40
4. Schematic of Electronic Devices	41
5. Facility Coordinate System	42
6. Schematic of Crossed Hot-Wire Probe Orientation	43
7. Crossed Hot-Wire Calibration, \bar{e} as a Function of $\overline{\rho u}$	44
8. Crossed Hot-Wire Calibration, \bar{A}_m as a Function of Re_{wt}	45
9. Crossed Hot-Wire Calibration, \bar{e}/\bar{E} as a Function of α	46
10. Crossed Hot-Wire Calibration, \bar{A}_v as a Function of Re_{wt}	47
11. Radial Profiles of Axial Velocity Turbulence Intensity for the Subsonic Jet	48
12. Radial Profiles of Radial Velocity Turbulence Intensity for the Subsonic Jet	49
13. Axial Distribution of Peak Mass Velocity Fluctuations, M = 2.5	50
14. Axial Distribution of Peak Radial Velocity Fluctuations, M = 2.5	51
15. Crossed Hot-Wire Mass Velocity Spectra in the Jet Shear Layer, M = 2.5	52
16. Crossed Hot-Wire Radial Velocity Spectra in the Jet Shear Layer, M = 2.5	53
17. Variation of Shear Layer Half-Thickness Parameter ($\delta/2d$) With Downstream Distance $\Delta M = 2.1$, $OM = 2.5$	54
18. Radial Distributions of Velocity Covariance, $\sqrt{u'v'}/\bar{u}$, M = 2.5	55

Figure	Page
19. Momentum Transport, $(\rho u)'v'$, Spectra in the Jet Shear Layer, Unexcited $M = 2.5$	56
20. Momentum Transport, $(\rho u)'v'$, Spectra in the Jet Shear Layer, Excited $M = 2.5$	57
21. Axial Distributions of Peak Mass Velocity and Peak Radial Velocity Fluctuations, $M = 2.1$	58
22. Radial Distributions of Velocity Covariance, $\sqrt{u'v'}/\bar{u}$, $M = 2.1$	59
23. Axial Distribution of Percent Coherent Structure, $\langle(\rho u)'\rangle_{rms}/(\rho u)'_{rms}$, in the Mass Velocity Fluctuations, $M = 2.5$	60
24. Wavelength Measurement of Axial Coherent Structure Oscillation, $M = 2.5$	61
25. Axial Distribution of Percent Coherent Structure, $\langle(\rho u)'v'\rangle_{rms}/[(\rho u)'v']_{rms}$, in the Velocity Covariance, $M = 2.5$	62

NOMENCLATURE

A_m	mass velocity fluctuation sensitivity coefficient
A_t	stagnation temperature fluctuation sensitivity coefficient
A_v	radial velocity fluctuation sensitivity coefficient
b	$(\gamma - 1) M^2 s$
d	effective nozzle exit diameter, nozzle exit diameter minus twice the displacement thickness
D	nozzle exit diameter
e	hot-wire voltage
E	$(e_1 + e_2)/2$, e_1 and e_2 evaluated at $\alpha = 0$
f	frequency (Hz)
$f(\vec{x}, t)$	general fluctuating quantity
k	complex wave number
k_i	imaginary part of the complex wave number
k_r	real part of the complex wave number
M	Mach number
P	pressure
P_{ch}	test chamber pressure
P_n	static nozzle exit pressure
r	radial distance from jet centerline, cylindrical coordinate system
R	radial distance from center of jet at nozzle exit, spherical coordinate system

Re	Reynolds number, $U_0 D/\nu$
R_w	hot-wire resistance
s	$[1 + ((\gamma - 1)/2) M^2]^{-1}$
St	Strouhal number, fd/U_0
t	time
T	temperature
T_w	hot-wire temperature
u	axial velocity
U_0	jet centerline exit velocity
v	radial velocity
x	downstream distance from the nozzle
\vec{x}	general spatial quantity
y	vertical distance from the nozzle
z	horizontal distance from the nozzle
α	yaw angle of the crossed hot-wire probe relative to the jet centerline
β	angular coordinate in spherical coordinate system
γ	ratio of specific heats
δ	local shear layer thickness
θ	azimuthal angle
ν	kinematic viscosity
λ	axial wavelength
ρ	density
τ	period of the wave
$()_t$	quantity evaluated at stagnation conditions
$()_0$	quantity evaluated at jet exit
$(\overline{\quad})$	time average of quantity

-
- < > phase average of quantity
 - ()' total fluctuation, ()' = (~) + ()"
 - ()" random portion of fluctuation
 - (~) periodic portion of fluctuation

CHAPTER I

INTRODUCTION

A. Background

In the past 25 years extensive research has been devoted to the study and control of the noise produced by high speed exhaust jets. Many ad hoc attempts have been made to control this noise, but still there is no completely satisfactory jet noise suppressor on commercial aircraft at this time. Clearly, if we are to develop effective jet silencers in the future, a thorough understanding of the jet noise generation processes is needed.

Early theoretical analyses of aerodynamic noise generation were able to approximately predict the radiated acoustic field if the distribution of acoustic sources within the jet flow were known (1) through (7). These theories provided considerable understanding of the noise generation processes. However, since the understanding of the actual flow fluctuations composing the source terms was limited, these efforts typically only resulted in simple scaling laws, particularly in supersonic jet noise analyses.

Originally, the flow fluctuations in turbulent free shear flows were considered to be completely random in nature. In recent years, however, a number of experimental studies have indicated that a coherent structure exists in these flows (8) through (11). It has also been hypothesized

that this organized structure which is large scale in nature, may be of fundamental importance in the noise generation processes (12) (13) (14).

Presently there is extensive debate over the description of the large scale disturbances. The works of Laufer et al. (15) and Lau et al. (11) among others interpret these coherent disturbances as vortex structures that tend to interact (pair) as they convect downstream. The process in which these structures interact has been proposed to be an important mechanism of subsonic jet noise generation (15) (16). Other researchers have attempted to model the organized fluctuations as instability waves (17) through (21). Of these theories, Morris and Tam (21) have developed the most comprehensive noise prediction model for supersonic jets. Their model can be used to calculate the noise generated by the large scale instability waves from a matched asymptotic expansion method. Their predictions are found to be in reasonable agreement with the experimental results of Yu and Dosanjh (22) for an $M = 1.5$ jet.

B. Subject of Research

Over the last few years, extensive experimental measurements have been performed in an ongoing high speed jet noise research program at Oklahoma State University (23) through (28). The major goals of this research were to provide understanding of the noise generation processes and to provide the experimental framework upon which more accurate jet noise theories could build. The measurements were concentrated on the flowfield and acoustic properties of high speed jets in the Mach number range from $M = 0.9$ to $M = 2.5$. A unique approach was taken to obtain most of these data in that the jets were operated at a low Reynolds number, in the range from $Re = 3700$ to $15,000$. Additional measurements

were performed at a moderate Reynolds number ($Re \approx 70,000$) most recently by Troutt (28).

Lowering the Reynolds number from that of conventional laboratory jets exhausting to the atmosphere ($Re \approx 1 \times 10^6$) produces several experimental advantages. The low density of the flows allows standard hot-wire anemometry techniques to be employed for measurement of the fluctuating flow properties. Also the small scale turbulence which tends to mask the coherent flow structure is decreased, making the structure's detection and characterization easier.

These experimental studies have shown that for low Reynolds number (transitional) supersonic jets there are instability waves present which can be characterized by a linear stability theory and that these instability waves produce a major portion of the noise radiated by the jet (23) (24). The noise produced by the instabilities was also found to have comparable amplitudes and directivity patterns to those of high Reynolds number jets. These results suggest that coherent flow disturbances in the form of instability waves are powerful noise generators and that the theoretical approach taken by researchers such as Tam (17), Liu (19), Morris (20), and Chan (18) holds promise.

Results of the low Reynolds number subsonic studies ($M = 0.9$) show comparable acoustic properties to those of a high Reynolds number fully turbulent jet. However, an interesting phenomenon in contrast to previous work with low Reynolds number supersonic jets was observed. The flow and acoustic fields were found to be dominated by quite different peak frequencies. This finding strongly indicates that the noise generation probably results from a mechanism different from that of a supersonic jet. In fact, Stromberg, McLaughlin, and Troutt (27) suggest that

the vortex pairing model proposed by Laufer et al. (15) might be appropriate for this subsonic jet.

The present study was intended primarily to extend the work done previously on the low Reynolds number ($Re < 10,000$) supersonic jets by Morrison and McLaughlin (25) (26). The approach has been to make more detailed flow and acoustic measurements in and around the major noise production region of the jets (i.e., near the end of the potential core). The chosen Mach number of the jets for a majority of the measurements was $M = 2.5$. It was considered experimentally advantageous to perform most of the measurements at this Mach number so that most of the transonic hot-wire problems were avoided.

C. Objectives

The overall goal of the present study was to increase the understanding of the flow processes in the noise producing region of supersonic jets with emphasis on the nonlinear processes and their role in the jet instability and turbulence development. In the future analysis of dominant jet instabilities and the resulting noise production, it will become increasingly desirable to quantify some of the important nonlinear processes.

Nonlinear processes* have two direct effects on the flow:

1. They broaden the spectral distribution of the fluctuations and produce high amplitude harmonics and subharmonics of the dominant spectral components.

*It should be noted that the primary nonlinear terms in the governing flow equations occur in the Reynolds stress tensor. The term $\rho \overline{u'v'}$ is the most important component, since it is responsible for the transport of x-momentum in the radial direction.

2. They increase the mixing (or simply the momentum transport) in the shear layer so as to have a direct effect on the mean flow properties.

Thus the specific objectives of this study are as follows:

1. To quantify and characterize some of the important nonlinear processes in the jet flow (i.e., the production of Reynolds stress).
2. To determine what portion of the flow fluctuations is attributable to random turbulence.
3. To obtain information relating the radiated noise to the flow fluctuations in order to gain more understanding of the dominant noise generating mechanisms.

Satisfying the above objectives would give valuable information concerning the significance of nonlinear instability interactions as well as test the appropriateness of a wave model description of the dominant jet fluctuations. Experimental evidence established from these measurements should also be helpful in the development of future instability/turbulence models.

CHAPTER II

EXPERIMENTAL APPARATUS

A. General Facility

The experiments in this study were performed in the Oklahoma State University free jet test facility shown in the schematic diagram of Figure 1 (see Appendix). This facility is unlike any other in the United States in that it allows experimental measurements of a jet to be made in a low pressure anechoic environment. The facility consists of three sections: a compressed air source and stilling chamber to supply the jet stream, a test chamber section, and a vacuum system to provide the low pressure environment.

Compressed air is supplied to the jet facility from a 1.8 cubic meter storage tank through a pressure regulator, a throttling valve, and a stilling section. The compressed air is dehumidified prior to storage and the compressor is shut down during the actual experimental measurements to eliminate extraneous vibrations to the system. The pressure regulator and throttling valve combination were used to control the stagnation pressure of the jet. The stilling section is 15 cm in diameter by 55 cm in length and consists of a 5 cm length of acoustical foam, three perforated plates, a 7.6 cm honeycomb section, and six fine mesh screens all to perform turbulence reduction and flow management.

A cubic contoured contraction section (area ratio greater than 200:1) connects the stilling section to the jet nozzle in the test

chamber. Several different axisymmetric supersonic nozzles were used in this study: design Mach number $M = 2.5$ with an exit diameter (D) of 9 mm, and Mach numbers $M = 2.1$ and $M = 1.4$ with exit diameters of 10 mm. The inviscid nozzle contours were determined using the method of characteristics to obtain a contour which gave uniform parallel flow at the nozzle exit (29). A boundary layer correction was also added corresponding to an average Reynolds number condition ($10,000 \leq Re \leq 20,000$).

The jet exhausts into a 0.7 x 0.8 x 1.2 meter vacuum chamber with a 5 cm thick Scott Pyrell acoustical absorption form liner. This combination produces an anechoic environment for frequencies above one kilohertz. The vacuum chamber is depicted in Figure 2.

This test chamber is equipped with a probe drive system capable of translation in three orthogonal directions (x, y, z) and rotation in the horizontal plane ($x-z$ plane). Precision ten-turn potentiometers incorporated in the system provide D.C. voltage readout proportional to the probe location. This system gives accurate and repeatable positioning of various sensor probes: normal hot-wire probe, crossed hot-wire probe, pitot pressure probe, static pressure probe, or condenser microphone. Another stationary probe may also be mounted above the jet in the vertical plane through the centerline.

Each jet nozzle is equipped with a glow discharge device which was used to artificially excite the jet. The method of excitation was similar to the technique reported earlier by Kendall (30) and was used in previous studies at Oklahoma State University (23) through (28). The excitation device consists of a 1.5 mm diameter tungsten electrode insulated with ceramic tubing and mounted within 2 mm of the nozzle exit. An oscillating glow discharge is established by applying an alternating

voltage biased to a large negative potential (-300 volts D.C.) to the electrode. The frequency of the alternating voltage can be varied using a signal generator, thus allowing a small controlled disturbance to be input to the jet.

The vacuum chamber has an exhaust diffuser with a variable throat which allows constant and accurate control of the pressure in the chamber. The diffuser is connected to a $0.1 \text{ m}^3/\text{sec}$ Kinney vacuum pump by way of 15 meters of piping and a 30 cubic meter vacuum storage tank. Thus pressure fluctuations and vibrations from the vacuum pump have a negligible effect on the test chamber environment.

B. Instrumentation

Pressure measurements were made with a silicone oil (specific gravity of 0.93) manometer and a mercury manometer, both referenced to a vacuum of 30 microns of mercury, absolute pressure. Pressure taps were located at various positions in the facility to measure stilling chamber stagnation pressure, nozzle static pressure, and test chamber pressure. By controlling both the stilling chamber stagnation pressure and the test chamber pressure, it was possible to obtain a perfectly expanded jet at a given Reynolds number over a wide range.

Acoustic measurements were made using a 3.175 mm diameter Brüel and Kjaer condenser microphone type 4138 and associated B & K type 2618 pre-amplifier and type 2804 power supply. The microphone has omnidirectional response within ± 3 dB for frequencies up to 60 kHz. Calibration of the microphone was performed in a low pressure environment using a B & K type 4220 piston phone. Previous studies have shown that the calibration is essentially independent of the ambient pressure (24).

Flow fluctuation measurements were made using DISA constant temperature anemometry electronics that consisted of a DISA 55M01 main frame with a 55M10 standard bridge (two anemometers were needed in crossed hot-wire measurements). The normal hot-wire probes were DISA 55A53 subminiature probes mounted on slender brass wedges. Crossed hot-wire probes were constructed from round jewelers broaches, perforated thermocouple ceramic insulators, and 5 micron diameter platinum-plated tungsten wire. These were also mounted on brass wedges. Normally the frequency response of the hot-wire probe (normal or crossed) and electronics was found to be near 60 kHz based on square wave response tests. For total level measurements both the hot-wire and microphone signals were band-pass filtered from 3 kHz to 60 kHz to remove chamber and electronic resonances. Construction details of the hot-wire probes are shown in the schematic diagram of Figure 3.

Using a technique similar to that given by Rose (31) (32) it was possible to simultaneously measure the instantaneous axial mass velocity fluctuations and radial velocity fluctuations from the crossed hot-wire probe (refer to the Experimental Procedures chapter). This required special electronics to instantaneously add and subtract the two crossed wire outputs. Using multiplication electronics it was also possible to obtain a component of the Reynolds stress tensor. These electronic configurations were constructed from commercially available analog devices and are detailed in the schematic diagram of Figure 4.

Frequency spectra of both the hot-wire and microphone signals were made using a Tektronix 7L5 spectrum analyzer. A constant bandwidth of one kilohertz was used to generate all spectra in this study. Correlation and phase-averaging of sensor signals were performed using a Saicor

model SAI 43A correlation and probability analyzer. Both instruments have frequency response in excess of 100 kHz and were considered adequate for this study.

CHAPTER III

EXPERIMENTAL PROCEDURES

A. General

The majority of the experimental measurements contained in this study were performed on a perfectly expanded (nozzle exit pressure P_n is maintained within 2% of jet back pressure P_{ch}) jet of nominal Mach number $M = 2.5$ and Reynolds number of approximately 8700. These conditions were chosen to correspond to those used in work done previously by Morrison and McLaughlin (25) (26). Additionally, jets of Mach number $M = 2.1$ and 1.4 were used in the calibration of the cross hot-wire probes. The stagnation temperature of the jets was room temperature (approximately 294 K).

A facility coordinate system (origin at the jet exit) used in all measurements is shown in Figure 5. Positioning within this coordinate system was done based on the effective jet diameter d and most of the data presented in this study is nondimensionalized using this diameter. The effective diameter is defined to be the physical jet exit diameter D , minus twice the displacement thickness of the boundary layer (the ratio D/d was 1.12 for the $M = 2.5$, $Re = 8700$ jet).

B. Crossed Hot-Wire Procedure and Data Analysis

The fluctuating properties (axial mass velocity and radial velocity) of the jet flow were obtained using a crossed hot-wire anemometry

technique similar to that given by Rose (31) (32). The validity of this data reduction procedure in supersonic flow requires that the Mach number of the flow normal to the hot-wire be above 1.2. A crossed hot-wire probe consists of wires inclined approximately 45 degrees to the mean flow direction; thus, detailed measurements were made primarily in the Mach number $M = 2.5$ jet and in regions of its flow where the Mach number normal to the wire satisfied this criterion.

All measurements using the crossed hot-wire were made with the probe located in the horizontal x - z plane of the jet. Figure 6 shows a schematic diagram detailing the proper orientation of the crossed hot-wire probe in a jet shear layer to measure the mean flow, the flow fluctuations in the axial direction, and the fluctuations in the radial direction. For comparison, the schematic also shows the orientation of a normal hot-wire probe for measuring the mean flow and flow fluctuations in the axial direction in the same shear layer.

Following the ideas of Morkovin and Phinney (33), the instantaneous voltage fluctuation measured from an inclined hot-wire in supersonic flow can be represented by the following expression:

$$\frac{e'}{\bar{e}} = A_m \frac{(\rho u)'}{\bar{\rho u}} + A_t \frac{T_t'}{\bar{T}_t} + A_v \frac{v'}{u}$$

where A_m , A_t , and A_v are the sensitivity coefficients for mass velocity fluctuations, total temperature fluctuations, and radial velocity fluctuations, respectively. These coefficients can be evaluated as follows (32).

$$A_m = \left. \frac{\partial \ln \bar{e}}{\partial \ln \frac{\rho u}{\bar{\rho u}}} \right|_{T_t, R_w, \alpha \text{ constant}}$$

$$A_t = \frac{\partial \ln \bar{e}}{\partial \ln \bar{T}_t} \bigg|_{\overline{\rho u}, R_w, \alpha \text{ constant}}$$

$$A_v = \frac{\partial \ln \bar{e}}{\partial \alpha} \bigg|_{\overline{\rho u}, R_w, T_t \text{ constant}}$$

Two oppositely inclined wires of a crossed hot-wire probe give outputs that can be instantaneously added and subtracted to result in

$$\begin{aligned} (e_1' + e_2') &= (\bar{e}_1 A_{m_1} + \bar{e}_2 A_{m_2}) \frac{(\rho u)'}{\overline{\rho u}} + (\bar{e}_1 A_{t_1} + \bar{e}_2 A_{t_2}) \frac{T_t'}{\bar{T}_t} \\ &\quad + (\bar{e}_1 A_{v_1} - \bar{e}_2 A_{v_2}) \frac{v'}{\bar{u}} \end{aligned}$$

$$\begin{aligned} (e_1' - e_2') &= (\bar{e}_1 A_{m_1} - \bar{e}_2 A_{m_2}) \frac{(\rho u)'}{\overline{\rho u}} + (\bar{e}_1 A_{t_1} - \bar{e}_2 A_{t_2}) \frac{T_t'}{\bar{T}_t} \\ &\quad + (\bar{e}_1 A_{v_1} + \bar{e}_2 A_{v_2}) \frac{v'}{\bar{u}} . \end{aligned}$$

For the crossed hot-wire measurements reported in this study, it was normally assumed that the total temperature fluctuations were negligible. Both Troutt (28) and Morrison (25) have determined that in supersonic jets at Reynolds numbers from 3700 to 70,000 total temperature fluctuations were typically responsible for less than 2 percent of the hot-wire rms voltage fluctuations, thus justifying the assumption. Also, the crossed hot-wires were matched so that the sensitivity coefficients A_m and A_v were approximately the same for each wire. These simplifications resulted in two voltages proportional to $(\rho u)' / \overline{\rho u}$ and v' / \bar{u} , respectively:

$$(e_1' + e_2') = (\bar{e}_1 A_{m_1} + \bar{e}_2 A_{m_2}) \frac{(\rho u)'}{\overline{\rho u}}$$

$$(e_1' - e_2') = (\overline{e_1 A_{v_1}} + \overline{e_2 A_{v_2}}) \frac{v'}{\bar{u}}.$$

Additionally, the major shear component of the Reynolds stress tensor was determined by multiplication of these voltages proportional to $(\rho u)'/\overline{\rho u}$ and v'/\bar{u} , and use of the following relationship derived by Rose (31) (32):

$$\frac{\overline{u'v'}}{\bar{u}^2} = \frac{s}{s+b} \frac{\overline{(\rho u)'v'}}{\bar{\rho} \bar{u}^2}$$

where

$$s = \frac{1}{1 + \frac{(\gamma - 1)}{2} M^2}$$

$$b = (\gamma - 1) M^2 s.$$

The required sensitivities in the above relations were evaluated by direct calibration over the range of Mach and Reynolds numbers encountered in this study. The calibration was performed by locating the crossed hot-wire probe on the centerline of the jet near the nozzle exit. The Reynolds number (and thus $\overline{\rho u}$) was varied by changing the upstream stagnation pressure. Different Mach numbers were obtained using three nozzles operating at respective design pressure ratios ($M = 1.4, 2.1,$ and 2.5).

The calibration of the crossed hot-wire was performed as follows. The probe was positioned in one of the nozzles to give the desired nominal calibration Mach number. With the probe at zero angle of incidence to the free stream flow direction, the mean bridge voltage \bar{e} was read from the anemometer for each wire for various values of stagnation pressure with T_t and T_w held constant. The results of these readings were

then plotted as shown for the three Mach numbers in Figure 7. (The data are plotted in dimensional terms here to show the actual results obtained from the calibration procedure.) The derivative $\partial \ln \bar{e} / \partial \ln \bar{\rho u}$ was needed to obtain the A_m sensitivity coefficient and the data of the figure were fitted with a second order curve to more readily accomplish this. There was an immeasurable effect of Mach number on the values of $\partial \ln \bar{e} / \partial \ln \bar{\rho u}$. Figure 8 shows the results of determining these sensitivity coefficients for each wire over the Reynolds number range of interest. (The data are presented as the average value of the two individual wire sensitivities.) Shown also for comparison are calibration data obtained by Morrison (25) in the same facility using a normal hot-wire and data obtained by Rose (32) with a normal hot-wire in a supersonic boundary layer. The data of Rose are substantially different, probably due to greater conduction end loss effects resulting from a low probe aspect ratio. (The length to diameter ratios for the various data are Morrison, $\ell/d = 200$, Rose $\ell/d = 100$, and present study $\ell/d = 250$.)

To obtain the sensitivity to angulation, A_v , the probe was rotated between $+5^\circ$ and -5° incidence angle to the free stream flow direction in increments of 1° using the facility probe drive system. Again at a desired calibration Mach number, the mean bridge voltage of the two wires \bar{e} was read for each position with the values of $\bar{\rho u}$, T_t , and T_w held constant. This procedure was repeated for various values of $\bar{\rho u}$. The results of these readings were plotted as shown in the example of Figure 9 and a linear regression scheme was used to determine the derivatives $\partial \ln \bar{e} / \partial \alpha$ needed for the A_v coefficients. (Note that the curves of Figure 9 do not intersect at the zero degree point as one might expect, due to inexact matching of the wires--slight differences in individual

wire output for identical flow conditions.) The sensitivity coefficients (again an average of the individual wire sensitivities) determined from these data are given in Figure 10 along with similar data obtained by Rose (32) using a single inclined hot-wire. The figure demonstrates a significant Mach number effect in this low Reynolds number flow regime and the results of differing conduction end loss effects can again be seen in the comparison with the data of Rose.

To decompose the crossed hot-wire voltages into the appropriate fluctuations, the local $\bar{\rho}\bar{u}$ was determined from the \bar{e} outputs at the given probe location and the local Mach number was determined from the mean flow data of Morrison (25) for the same jet flow. These quantities were then used with the previously discussed calibration curves to calculate the appropriate sensitivity terms.

C. Phase-Averaging Procedure

Turbulent flows with an inherent coherent structure lend themselves to a triple decomposition of the type:

$$f(\vec{x},t) = \bar{f}(x) + \tilde{f}(\vec{x},t) + f''(\vec{x},t).$$

In this representation (first used by Kendall (34) and Hussain and Reynolds (35)), any flow quantity consists of a sum of the mean flow $\bar{f}(\vec{x})$, the organized wave $\tilde{f}(\vec{x},t)$, and the random turbulence $f''(\vec{x},t)$.

The mean flow portion is given by the conventional time average of $f(\vec{x},t)$:

$$\bar{f}(\vec{x}) = \lim_{T \rightarrow \infty} \frac{1}{T} \int_0^T f(\vec{x},t) dt$$

In order to extract the periodic wave component from the total flow fluctuation, the phase-average of $f(\vec{x}, t)$ can be defined as

$$\langle f(\vec{x}, t) \rangle = \lim_{N \rightarrow \infty} \frac{1}{N} \sum_{n=0}^N f(\vec{x}, t + n\tau)$$

where τ is the period of the organized wave and N is the number of wave cycles over which the phase-average is taken. The phase-average of a single turbulent quantity is zero. Thus, the periodic wave component can be obtained from the phase-average of the total flow quantity by subtracting the mean flow contribution:

$$\tilde{f}(\vec{x}, t) = \langle f(\vec{x}, t) \rangle - \bar{f}(\vec{x}).$$

To effectively phase-average a fluctuating signal representing a flow quantity, a reference signal oscillating at the wave frequency must be supplied as a triggering source to initiate the measurement. For the measurements presented in this study, the signal supplied to the oscillating glow discharge device was used as the phase-averaging trigger. This is essentially the same procedure used by Hussain and Reynolds (35) to obtain $\tilde{f}(\vec{x}, t)$.

CHAPTER IV

EXPERIMENTAL RESULTS

A. Crossed Hot-Wire Measurements

A.1 Preliminary Subsonic Flowfield Measurements

In view of the absence of pertinent published fluctuating flow data for a supersonic jet obtained from an inclined hot-wire, preliminary crossed hot-wire measurements were made in a low-speed jet--for which considerably more published data exist--to assess the validity of the experimental technique and data reduction schemes discussed in the Experimental Procedures section. Comparisons of radial profiles of turbulence intensity for two axial locations obtained by this method in a one-inch diameter $Re = 30,000$, $M = 0.05$ jet are made in Figures 11 and 12 with those obtained by Bradshaw et al. (36) for a $Re = 300,000$, $M = 0.3$ jet. (Additionally, Seiner (37) has obtained results in favorable agreement with Bradshaw for a similar jet flow.) The fluctuating velocities are normalized based on the jet exit velocity, u_0 , and the radial and axial distances by the nozzle radius, r_0 . The results of Bradshaw exhibit turbulence levels that are generally lower than those of the present study; however, the curves follow closely the same trends. The results indicate the jet of the present study develops somewhat faster than the jet flow studied by Bradshaw. This would be expected for the more abrupt contraction section and lack of turbulence reduction material in the

stilling section of the facility used here. (The area contraction ratio here is approximately 9:1 whereas the facility used by Bradshaw had a contraction ratio greater than 36:1.) Bushnell (38) has found that at low Reynolds number there is a pronounced increase in turbulent fluctuations near the end of transition and beginning of turbulent flow in a boundary layer. This low Reynolds number effect is suspected to occur in free shear flows also and may give a partial explanation of the discrepancies seen in these data. Additionally, differences may be due in part to the fact that the present measurements did not use a linearizer preceding the rms voltmeter, as is normally standard practice in subsonic flow measurements.

These findings in the low-speed jet provide sufficient evidence that the previously detailed experimental procedure is capable of producing measurements of fluctuating flow quantities with reasonable accuracy. With this impetus, it was considered justifiable to pursue the desired measurements in the supersonic jets using the same techniques.

A.2 Flowfield Measurements, Mach Number 2.5 Jet

Crossed wire measurements have been attempted once before in our laboratory by Morrison (25). Unfortunately, older hot-wire electronics were used and their frequency response, in conjunction with the crossed hot-wire in the low Reynolds number supersonic jet flow, was not adequate. Consequently, his results were only of a preliminary nature.

The crossed hot-wire probe was used to measure the axial mass velocity and radial velocity fluctuation amplitudes in the various supersonic jets. Figure 13 shows the peak axial mass velocity fluctuation amplitude (normalized based on the local mean mass velocity) for an unexcited

$M = 2.5$, $Re = 8700$ jet as a function of axial location, x/d . The radial locations of the peak fluctuation amplitude corresponded to the center of the shear layer until the end of the potential core where the peak was found to be near the jet centerline. The figure contains data from two different experimental runs on separate days, as well as similar data obtained by Morrison (25) using a normal hot-wire probe in the same $M = 2.5$ jet. Uncertainty estimates based on instrumentation and calibration inaccuracies are shown as brackets on the data of the figure (and other figures that follow as well). These uncertainty estimates do not include consideration of inaccuracies due to probe resolution discussed later. Comparison shows that the data of the present study is some two to three times lower in fluctuation amplitude than the results of Morrison. The initial level of fluctuations measured using the crossed hot-wire probe is less than 0.2 percent ($2\frac{1}{2}$ times lower than that measured by Morrison). The amplitude of the fluctuations grows exponentially for the first 15 diameters downstream and peaks at a fluctuation level of approximately 16 percent near the axial location of the potential core end. Morrison has found that this exponential growth can be characterized by a linear stability type representation* with a growth rate, $-k_j d$, of 0.29 ± 0.04 (95% confidence interval). Although they are substantially low in amplitude, the measurements of the present study follow this calculated growth rate and other general trends closely.

*A linear stability analysis assumes a representation of the flow disturbance $Q(x,r,\theta,t)$ in the form: $Q(x,r,\theta,t) = \hat{Q}(r) \text{Re}\{\exp[i(k_r x - \omega t + n\theta) - k_j x]\}$ where Re here stands for the real part of { }, x , r , and θ are the axial, radial, and azimuthal coordinates, respectively.

Figure 14 shows the corresponding growth of the radial velocity fluctuations measured from the crossed hot-wire probe. The radial velocity fluctuations (normalized based on the local mean velocity) grow approximately exponentially from $x/d = 5$ to 20. The rate of growth, $-k_r d$, in this region is 0.19 ± 0.04 with a peak fluctuation level of 11 percent at $x/d = 25$. Measurements made by Lau et al. (39) in several different Mach number jets (including a $M = 1.4$ jet) using a laser velocimeter indicate that the radial velocity fluctuations are generally somewhat lower in amplitude than the corresponding axial velocity fluctuations. The measurements made using the crossed hot-wire also indicate this trend. However, because of the relative infancy of the use of laser velocimetry in supersonic flow measurements, in particular in the measurement of turbulence quantities, the associated uncertainties in these measurements are also substantial and absolute comparisons with these data are difficult to make. As previously pointed out, the axial mass velocity fluctuation measurements are substantially low in amplitude and the deterministic cause probably also affects measurements of the radially velocity somewhat.

Frequency spectra of the crossed hot-wire signal proportional to the mass velocity fluctuations obtained from the radial position of maximum voltage fluctuation (approximately at the center of the jet shear layer) are shown in Figure 15 for several x/d locations. Frequencies are presented in terms of the nondimensional Strouhal number, $St = fd/U_0$, where U_0 is the exit velocity of the jet and d is the effective diameter. The figure indicates that there is a band of unstable frequencies present with a majority of the fluctuations centered around the prevalent Strouhal number 0.16 spectral component. These spectra are very similar

in shape and development to those obtained by Morrison (25) in the same jet flow using a normal hot-wire. Figure 16 shows the corresponding crossed hot-wire spectra of the signal proportional to the radial velocity fluctuations for several x/d locations. These spectra contain a band of frequency components between $St = 0.04$ and $St = 0.35$, as in the mass velocity spectra of Figure 14. At $x/d = 5$, although the $St = 0.16$, spectral component is present as in the mass velocity spectra, a dominant peak at $St = 0.10$ is apparent. However, by $x/d = 10$, the $St = 0.16$ spectral component again dominates the spectrum. For the most part, these spectra show the same overall characteristics as the mass velocity spectra do.

In summary, mass velocity fluctuation amplitude measurements made using the crossed hot-wire probe are substantially low in comparison to previous data obtained in the same facility and flowfield using a normal hot-wire. The underlying cause of this discrepancy appears also to affect subsequent measurements of the radial velocity fluctuations. Figure 13, however, seems to demonstrate that the crossed wire measures an approximately correct axial distribution of the mass velocity fluctuations (with an attenuation of about 2). Additionally, spectra of the flow fluctuations are in reasonable agreement with previous results and thus indications are that the problem lies in the amplitude measurement technique and/or data reduction scheme and not in the frequency response of the instrument.

The suspected failing in these measurements is poor probe resolution. Measurements in the subsonic jet (where the ratio of jet diameter to probe size was approximately 17:1) using the described techniques proved to give quite reasonable results. In the measurements in the

M = 2.5 jet, however, the probe resolution was lower by a factor of almost three (ratio of jet diameter to probe size was approximately 6:1). Experience shows that this ratio should normally be much greater than this to obtain good resolution in the measurements. Also, in comparison to similar measurements made using a normal hot-wire, there is a difference in probe size on the order of 300:1 between it and the crossed hot-wire probe used here. (This can be seen clearly in the schematic diagram detailing both probes in Figure 6.) Originally the measurements of this study were to be performed in jets two times larger in diameter, thus giving the needed probe resolution; but lack of pumping capability in the jet facility limited the measurements to the smaller jets for the present time. Additional evidence of the probe resolution problem is given in the mass velocity measurements of Figure 13. The discrepancy between the crossed hot-wire measurements and the results of Morrison (25) decreases with increasing axial location. The results are lower by a factor of almost three near the nozzle exit, yet are only low by a factor of 1.7 past the end of the jet potential core where jet spreading gives a much larger flowfield. These results indicate that improved probe resolution should yield substantially better flow fluctuation amplitude measurements.

The emphasis in performing the measurements in this study centers on the development of the nonlinear processes in the jet, in particular on the production of Reynolds stresses. One of the dramatic results of the onset of nonlinear effects can be seen in the mean flow data of Morrison (25). Figure 17 shows how the local shear layer half thickness $\delta/2$ varies with axial location for two jet Mach numbers of interest. The location where the jet begins to widen at a faster rate coincides

approximately with the end of the potential core and is the point at which significant nonlinear interactions become important in the jet development. Additionally, spectral broadening of the flow fluctuations in this region is also evidence of strong nonlinear interactions.

Typical distributions of the axial and radial velocity covariance, expressed in terms of $\sqrt{\overline{u'v'}}/\bar{u}$ are shown in Figure 18. The curves show reasonable trends, but as before, the data appear to be low in amplitude. The laser velocimeter measurements of Lau et al. (39) in a $M = 1.4$ jet show a peak value for $\sqrt{\overline{u'v'}}/\bar{u}$ of approximately 0.10. This would indicate that the discrepancy in amplitude is of the same order as that found in the results of the mass velocity fluctuation measurements. Arguments have been put forward that the major cause of the amplitude discrepancy is the inadequate probe resolution. Despite this problem, the crossed wire measurements do provide some valuable insights into the flow processes in the developing jet. Figure 18 shows that the velocity fluctuation covariance $\overline{u'v'}$ undergoes a substantial change from $x/d = 15$ to $x/d = 20$ in the $M = 2.5$ jet. Not only has the peak value more than doubled, but the distribution has a substantially increased radial spread. This clearly demonstrates that this important nonlinear transport quantity has considerably more influence at $x/d = 20$ in comparison with $x/d = 15$. The change in the contribution of the Reynolds stress component $\overline{u'v'}$ from $x/d = 15$ to $x/d = 20$ coincides with the saturation and initial decay of the mass velocity fluctuations as depicted in Figure 12. It is also in this region where the mean flow begins to change substantially (refer to Figure 17). The combined evidence indicates that at $x/d = 15$ nonlinear effects (as measured in terms of $\overline{u'v'}$) become important and by $x/d = 20$ they are a major effect. This region of the $M = 2.5$ jet flow

has been shown by Morrison and McLaughlin (25) (26) to be one of dominant noise production in this jet.

Figure 19 contains spectra of the momentum transport $[(\rho u)'v']$ fluctuations for an unexcited (natural) $M = 2.5$ jet. These spectra were obtained in the approximate center of the jet shear layer where the velocity fluctuations maximize. As might be expected, the spectra contain a broad band of fluctuations centered at the approximate double frequency of the fundamental $St = 0.16$ instability. Beyond $x/d = 16$ the amplitude of the fluctuations increase noticeably and the spectra shift towards lower frequency content with downstream location as indicated by the spectrum at $x/d = 18$. Again these changes occur in the region of the end of the potential core where a major portion of the noise is being produced by the jet. Spectra of the momentum transport fluctuations for the same $M = 2.5$ jet flow excited at the $St = 0.16$ instability are shown in Figure 20. The spectra show that the excitation frequency plus integer multiples of that frequency. (It is difficult to ascertain the fundamental frequency in these spectra. The expected fundamental would be at $St = 0.32$ due to doubling of the $St = 0.16$ instability present in the mass velocity and radial velocity fluctuation when they are multiplied in the momentum transport quantity $[(\rho u)'v']$, but this is not clearly the case here.) The excited disturbances begin to grow noticeably past $x/d = 12$ and between $x/d = 14$ and $x/d = 16$ there is a substantial increase in the broad band fluctuations. By $x/d = 18$ the excited disturbances are virtually indistinguishable from the broad band components. These spectra give an indication that the coherent instability is present, at least to some degree, in some of the major nonlinear processes in the jet, namely in the momentum transport $[(\rho u)'v']$.

A.3 Flowfield Measurements, Mach Number 2.1 Jet

The growth of the mass velocity and radial velocity fluctuations determined using a crossed hot-wire are shown in Figure 21 for an unexcited $M = 2.1$, $Re = 7900$ jet. Also shown are similar mass velocity data obtained by Morrison (25) using a normal hot-wire in the same jet flow. Again, as in the case of the previous measurements performed on the $M = 2.5$ jet, the measurements for this jet are considerably low in amplitude. The mass velocity fluctuations increase approximately exponentially for the first six to seven diameters of flow, as do the measurements of Morrison, yet the peak fluctuation amplitude of 12.5 percent at $x/d = 10$ is only half of the value determined by Morrison. Correspondingly, the radial velocity fluctuations grow exponentially with a peak level attained at $x/d = 10$ of 8.6 percent. The explanation of the discrepancy in these data is as before in the $M = 2.5$ jet; poor resolution (ratio of nozzle diameter to probe size here is 7:1) results in fluctuation amplitude data low by a factor of at least two.

Figure 22 presents distributions of the axial and radial velocity covariance for several x/d locations. Again, the general trends appear to be reasonable, but the absolute amplitude values are suspect due to the probe resolution problem. The data show a peak value for the covariance, $\sqrt{u'v'}/\bar{u}$, of 0.04 at $x/d = 10$ (this is the approximate peak value obtained for the $M = 2.5$ jet also). Again, as in the $M = 2.5$ jet data, the velocity fluctuation covariance undergoes a major change in the region of the potential core end where the mean flow changes (refer to Figure 17) and the mass velocity fluctuations saturate and begin to decay. This corresponds also to the major noise production region of this $M = 2.1$ jet.

A.4 Summary of Crossed Hot-Wire Results

The original intent of the crossed hot-wire measurements in this study was to investigate some of the significant nonlinear interactions in the jet (i.e., investigate the development of the axial and radial velocity covariance component of the Reynolds stress tensor in the major noise producing regions of the jet flow near the end of the potential core). This study showed major difficulties in accurately determining flow fluctuation amplitude measurements from the crossed hot-wire in the present jet facility. However, the measurements did show qualitatively that the major nonlinear processes (as measured by the velocity covariance $\overline{u'v'}$) become important in the developing jet flow in the region of the end of the potential core where a majority of the noise is being produced.

B. Phase-Average Measurements

The fraction of organized structure present in the mass velocity fluctuations was measured by phase-averaging the signal from a normal hot-wire using the technique described in the Experimental Procedures section. Figure 23 shows the axial variation in the coherent fraction of the mass velocity fluctuations in the noise producing region of the excited $M = 2.5$, $Re = 8700$ jet. Each point represents a numerical average of all data taken at various radial locations for that particular axial position. The figures shows a distinct oscillation with axial location in the fraction of coherent structure. Morrison (25) performed this measurement for several axial locations, but his measurements were not in sufficient detail to establish this behavior. (The Morrison data are shown also in Figure 23 and are somewhat higher than the data of the

present study. This can be attributed to the fact that the peak values of the coherence are not shown for each axial position; instead average values across the jet for that location are shown.) The major point of note in these measurements is the strong decay in the coherence level (i.e., the disintegration of the coherent instability) past the end of the potential core. Additional detailed measurements were made between $x/d = 12$ and $x/d = 16$ on the jet centerline to determine the wavelength of this oscillation and are presented in Figure 24. The data show the axial wavelength to be approximately $\lambda/d = 2.25$. Comparison with the axial distribution of centerline Mach number shows this wavelength to correspond closely to the jet spatial wave cell structure (a system of weak expansion and compression waves caused by nonparallel flow at the nozzle exit) wavelength. Measurements of the variation in mean hot-wire voltage along the jet centerline verified the cell structure wavelength to be approximately $\lambda/d = 2.25$ also. Similar detailed measurements by Stromberg (27) in a subsonic jet showed no behavior of this sort.

Figure 25 shows the fraction of organized structure present in the signal proportional to the axial and radial velocity covariance as a function of downstream position. The level of coherence is much smaller than in the mass velocity fluctuations, as might be expected due to the interaction of spectral components in the velocity fluctuations to produce harmonics and subharmonics. However, it is of sufficient level to indicate the presence of some kind of coherent flow disturbance. An interesting feature of these data is the marked increase and then rapid decline of the coherence level in the vicinity of the potential core end.

In summary, the phase-average measurements of mass velocity fluctuations show some kind of spatial wave cell structure/flow disturbance

interaction to occur in the excited jet development. The measurements also indicate the fraction of coherent structure decreases as the flow progresses downstream and that there is a significant drop in the level after the potential core end. Phase-average measurements of the covariance along with previous spectra of the excited jet fluctuations show the presence of a coherent disturbance in some of the important non-linear jet interactions.

CHAPTER V

CONCLUSIONS

A. Summary

Crossed hot-wire measurements were performed in several supersonic jets of Mach number $M = 2.5$ and $M = 2.1$ at a low Reynolds number ($Re < 10,000$). The overall goal of the study was to increase the basic understanding of the flow processes in the noise producing regions of the jets by making detailed flow measurements there. The emphasis in the study centered on the nonlinear processes of the flow and their role in the jet instability and turbulence development. The major results derived from the study are listed as follows:

1. Preliminary measurements in a subsonic jet using the discussed crossed hot-wire technique gave results very close to previously published data, thus demonstrating the validity of the technique.

2. Measurements of the mass velocity and radial velocity fluctuations in the low Reynolds number supersonic jets were low in amplitude by a factor of two to three from previously reported data in the same flows, but basic trends such as growth rates and jet development remained the same.

3. Spectra of the flow fluctuations from the crossed hot-wire signals showed similar frequency content as previous work (shear layer fluctuations centered around the dominant $St = 0.16$ spectral component for the $M = 2.5$ jet).

4. Initial attempts at determining a component of the Reynolds stress tensor, $\sqrt{u'v'}/u$, from the crossed hot-wire measurements proved somewhat successful in that basic trends in the data were reasonable, but again the absolute amplitudes were low and suffered from a problem attributed to poor probe resolution. The measurements did however provide information demonstrating that there is a major change in the contribution of the Reynolds stress to the jet development in the region of the end of the potential core. It has been shown that this is the region where the mean flow changes dramatically, the flow fluctuations saturate and decay, and a major portion of the noise is being produced.

5. Detailed measurements of the fraction of coherent structure in the noise producing region of an excited $M = 2.5$ jet ($x/d = 12$ to $x/d = 20$) showed that some kind of spatial wave cell structure/flow disturbance interaction was present. The measurements also indicated that there is a substantial decrease in the coherence level past the end of the potential core.

6. Spectra and measurements of the fraction of coherent structure in the signal proportional to the Reynolds stress component showed that a coherent disturbance is indeed present in some of the nonlinear jet interactions.

7. Experience useful in future experimental efforts using crossed hot-wire techniques in supersonic jets was gained.

B. Recommendations for Further Study

The overshadowing difficulty with the measurements of this study was the lack of good probe resolution that prevented the desired detailed investigation of the flow processes. Originally the measurements were to

be made in an improved jet facility to overcome part of this problem, but a lack of pumping capability dictated the use of smaller jets thus creating the difficulty. Future efforts in this research will be conducted in a facility with greatly increased pumping capability, thus substantially better measurements can be made using the same techniques detailed here.

A viable program to continue this particular research should include a number of improvements:

1. The present pumping facility should be overhauled and evaluated as to its suitability for operating larger-size jets to obtain better probe resolution.

2. An evaluation should be made of the current crossed hot-wire probes. Smaller probes could possibly be constructed to improve probe resolution. An alternative might be to evaluate the suitability (and associated difficulties) of using the smaller-sized split-film sensor probes commercially available in place of the crossed hot-wire.

3. The present electronics associated with the determination of the flow quantities from the crossed wire should be rebuilt to give better accuracy and reliability.

4. Future efforts in this research should probably also include a program to utilize advanced digital data acquisition and processing techniques. Complicated experimental measurements of this nature are difficult to perform using on-line analog electronic equipment. The School of Mechanical and Aerospace Engineering at Oklahoma State University has an existing mini-computer facility (INTERDATA 7/16) suitable for this purpose. A program of this type would utilize the School's Honeywell 7600 FM tape deck for recording hot-wire signals during an experimental

run. (The data could later be digitized and analyzed using the mini-computer.) This plan will require more analog to digital conversion equipment to obtain the desired accuracy in the data reduction.

Additional advantages are also gained in utilizing a program of this type. Use of the computer greatly aids in the ease, speed, and accuracy of basic data reduction. This also enhances the possibility of using conditional sampling procedures in future work that should provide more insight into the physics of the jet flow.

BIBLIOGRAPHY

- (1) Lighthill, M. J. "On Sound Generated Aerodynamically, I General Theory." Proc. Roy. Soc., A211 (1952), pp. 546-587.
- (2) Lighthill, M. J. "On Sound Generated Aerodynamically, II Turbulence as a Source of Sound." Proc. Roy. Soc., A222 (1954), pp. 1-32.
- (3) Ffowcs Williams, J. E. "The Noise From Turbulence Convected at High Speed." Phil. Trans. Roy. Soc., A255 (1963), p. 459.
- (4) Phillips, O. M. "On the Generation of Sound by Supersonic Turbulent Shear Layer." J. Fluid Mech., Vol. 9 (1960), pp. 1-28.
- (5) Ribner, H. S. "The Generation of Sound by Turbulent Jets." Advances in Applied Mechanics, Vol. 8 (1964), pp. 103-182.
- (6) Pao, S. P., and M. V. Lawson. "Some Applications of Jet Noise Theory." AIAA Paper No. 70-233, 1970.
- (7) Lilley, G. M., P. Morris, and B. J. Tester. "On the Theory of Jet Noise and Its Applications." AIAA Paper No. 73-987, 1973.
- (8) Brown, G., and A. Roshko. "The Effect of Density Difference on the Turbulent Mixing Layer." AGARD Conference on Turbulent Shear Flows. Conf. Proc. No. 93 (1971), p. 23.
- (9) Winant, C. D., and F. K. Browand. "Vortex Pairing, the Mechanism of Turbulent Mixing Layer Growth at Moderate Reynolds Number." J. Fluid Mech., Vol. 63 (1974), pp. 237-256.
- (10) Crow, S. C., and F. H. Champagne. "Orderly Structure in Jet Turbulence." J. Fluid Mech., Vol. 48 (1971), pp. 547-591.
- (11) Lau, J. C., M. J. Fisher, and H. V. Fuchs. "The Intrinsic Structure of Turbulent Jets." J. Sound and Vibration, Vol. 22, No. 4 (1972), pp. 379-406.
- (12) Mollo-Christensen, E. "Jet Noise and Shear Flow Instability Seen From an Experimenter's Viewpoint." J. Appl. Mech., Vol. 34 (1967), pp. 1-7.
- (13) Bishop, K. A., J. E. Ffowcs Williams, and W. Smith. "On the Noise Sources of the Unsuppressed High-Speed Jet." J. Fluid Mech., Vol. 50 (1971), pp. 21-31.

- (14) Tam, C. K. W. "On the Noise of a Nearly Ideally Expanded Supersonic Jet." J. Fluid Mech., Vol. 51 (1972), pp. 69-95.
- (15) Laufer, J., R. E. Kaplan, and W. T. Chu. "On the Generation of Jet Noise." AGARD Conference Proceedings No. 131 on Noise Mechanisms, 1973.
- (16) Ffowcs Williams, J. E., and A. J. Kempton. "The Noise From the Large-Scale Structure of a Jet." J. Fluid Mech., Vol. 84 (1976), pp. 673-694.
- (17) Tam, C. K. W. "Supersonic Jet Noise Generated by Large-Scale Disturbances." J. Sound and Vibration, Vol. 38 (1974), pp. 51-79.
- (18) Chan, Y. Y. "Discrete Acoustic Radiation From a High-Speed Jet as a Singular Perturbation Problem." Canadian Aeronautics and Space Journal, Vol. 38 (1974), pp. 51-79.
- (19) Liu, J. T. C. "Developing Large-Scale Wavelike Eddies and the Near Jet Noise Field." J. Fluid Mech., Vol. 62 (1974), pp. 437-464.
- (20) Morris, P. J. "Flow Characteristics of the Large-Scale Wavelike Structure of a Supersonic Round Jet." J. Sound and Vibration, Vol. 53 (1977), pp. 223-244.
- (21) Morris, P. J., and C. K. W. Tam. "Near and Far Field Noise From Large-Scale Instabilities of Axisymmetric Jets." AIAA Paper No. 77-1351, 1977.
- (22) Yu, J. C., and D. S. Dosanjh. "Noise Field of Supersonic Mach 1.5 Cold Jet." J. Acoust. Soc. Am., Vol. 51 (1973), pp. 1400-1410.
- (23) McLaughlin, D. K., G. L. Morrison, and T. R. Troutt, "Experiments on the Instability Waves in a Supersonic Jet and Their Acoustic Radiation." J. Fluid Mech., Vol. 69 (1976), pp. 73-95.
- (24) McLaughlin, D. K., G. L. Morrison, and T. R. Troutt. "Reynolds Number Dependence in Supersonic Jet Noise." AIAA J., Vol. 15 (1977), pp. 526-532.
- (25) Morrison, G. L. "Flow Instability and Acoustic Radiation Measurements of Low Reynolds Number Supersonic Jets." (Unpublished Ph.D. thesis, Oklahoma State University, Stillwater, Oklahoma, 1977.)
- (26) Morrison, G. L., and D. K. McLaughlin. "The Noise Generation by Instabilities in Low Reynolds Number Supersonic Jets." J. Sound and Vibration (to be published).
- (27) Stromberg, J. L., D. K. McLaughlin, and T. R. Troutt. "Flowfield and Acoustic Properties of a Mach Number 0.9 Jet at a Low Reynolds Number." AIAA Paper No. 79-0593, 1979.

- (28) Troutt, T. R. "Measurements on the Flow and Acoustic Properties of a Moderate Reynolds Number Supersonic Jet." (Unpublished Ph.D. thesis, Oklahoma State University, Stillwater, Oklahoma, 1978.)
- (29) Johnson, C. B., and L. R. Boney. "A Method for Calculating a Real-Gas Two-Dimensional Nozzle Contour Including the Effects of Gamma." NASA TM X-3243, Langley Research Center, Hampton, Virginia, 1975.
- (30) Kendall, J. M. "Supersonic Boundary Layer Stability Experiments." Proceedings of the Boundary Layer Transition Study Group Meeting, Vol. II, Aerospace Report No. TR-0158 (S3816-63)-1, 1967.
- (31) Johnson, D. A., and W. C. Rose. "Laser Velocimeter and Hot-Wire Anemometer Comparison in a Supersonic Boundary Layer." AIAA J., Vol. 13, No. 4 (1975), pp. 512-515.
- (32) Rose, W. C. "The Behavior of a Compressible Turbulent Boundary Layer in a Shock-Wave-Induced Adverse Pressure Gradient." NASA TN D-7092, 1973.
- (33) Morkovin, M. V., and R. E. Phinney. "Extended Applications of Hot-Wire Anemometry to High-Speed Turbulent Boundary Layers." AFOSR TN-58-469, Johns Hopkins Univ., Dept. of Aeronautics, June, 1958.
- (34) Kendall, J. M. "The Turbulent Boundary Layer Over a Wall With Progressive Surface Waves." J. Fluid Mech., Vol. 41 (1970), pp. 259-281.
- (35) Hussain, A. K. M. F., and W. C. Reynolds. "The Mechanics of an Organized Wave in Turbulent Shear Flow." J. Fluid Mech., Vol. 41 (1970), pp. 241-258.
- (36) Bradshaw, P., D. H. Ferriss, and R. H. Johnson. "Turbulence in the Noise Producing Region of a Circular Jet." J. Fluid Mech., Vol. 19 (1964), pp. 591-624.
- (37) Seiner, J. M. "The Distribution of Jet Source Strength Intensity by Means of a Direct Correlation Technique." (Unpublished Ph.D. thesis, Pennsylvania State University, University Park, Pennsylvania, 1974.)
- (38) Bushnell, D. M. "Calculation of Turbulent Free Mixing--Status and Problems." Free Turbulent Shear Flows Vol. I Conference Proceedings, NASA SP-321, 1972.
- (39) Lau, J. C., P. J. Morris, and M. J. Fisher. "Turbulence Measurements in Subsonic and Supersonic Jets Using a Laser Velocimeter." AIAA Paper No. 76-348, 1976.

APPENDIX

FIGURES

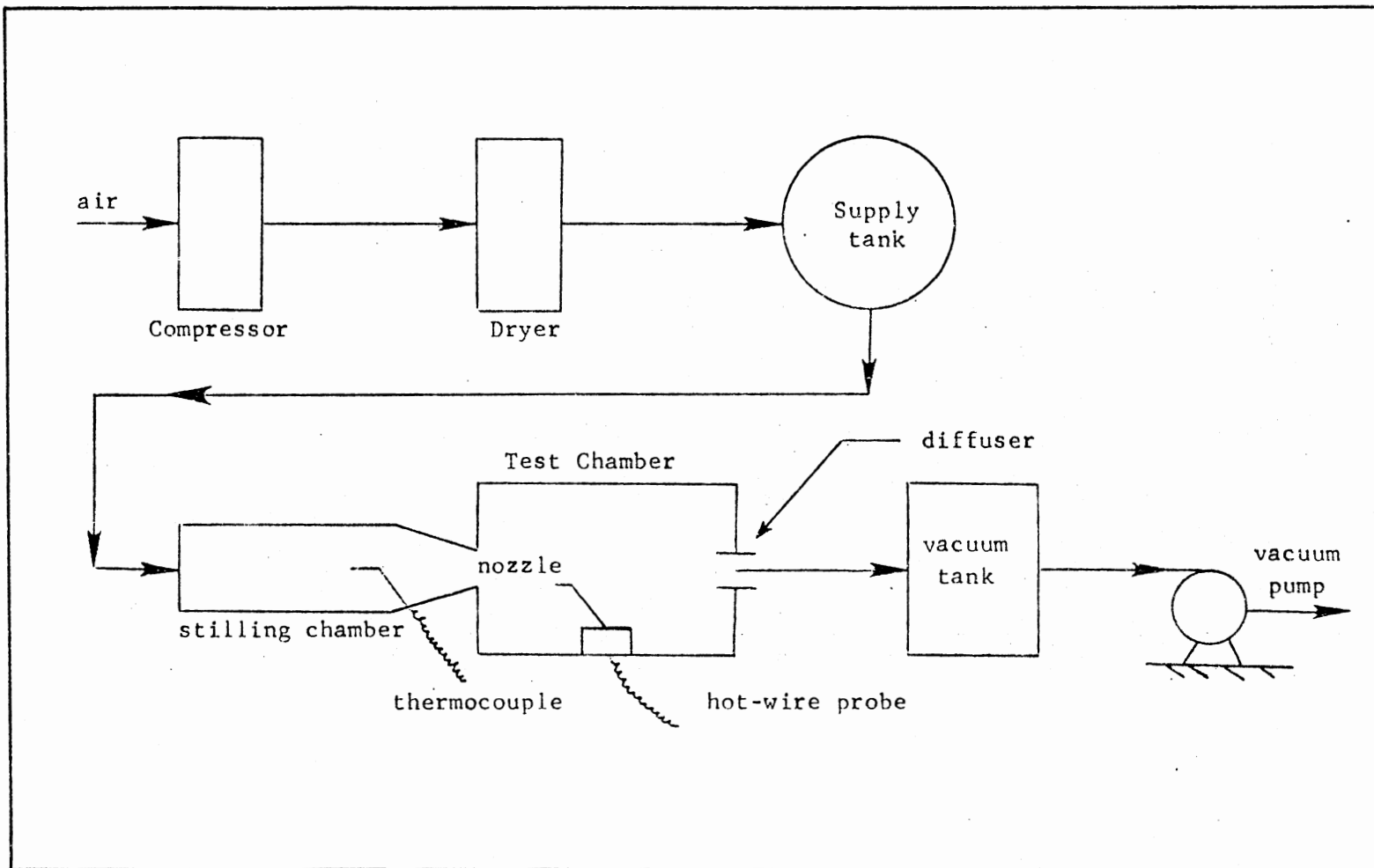


Figure 1. Schematic of Overall Facility

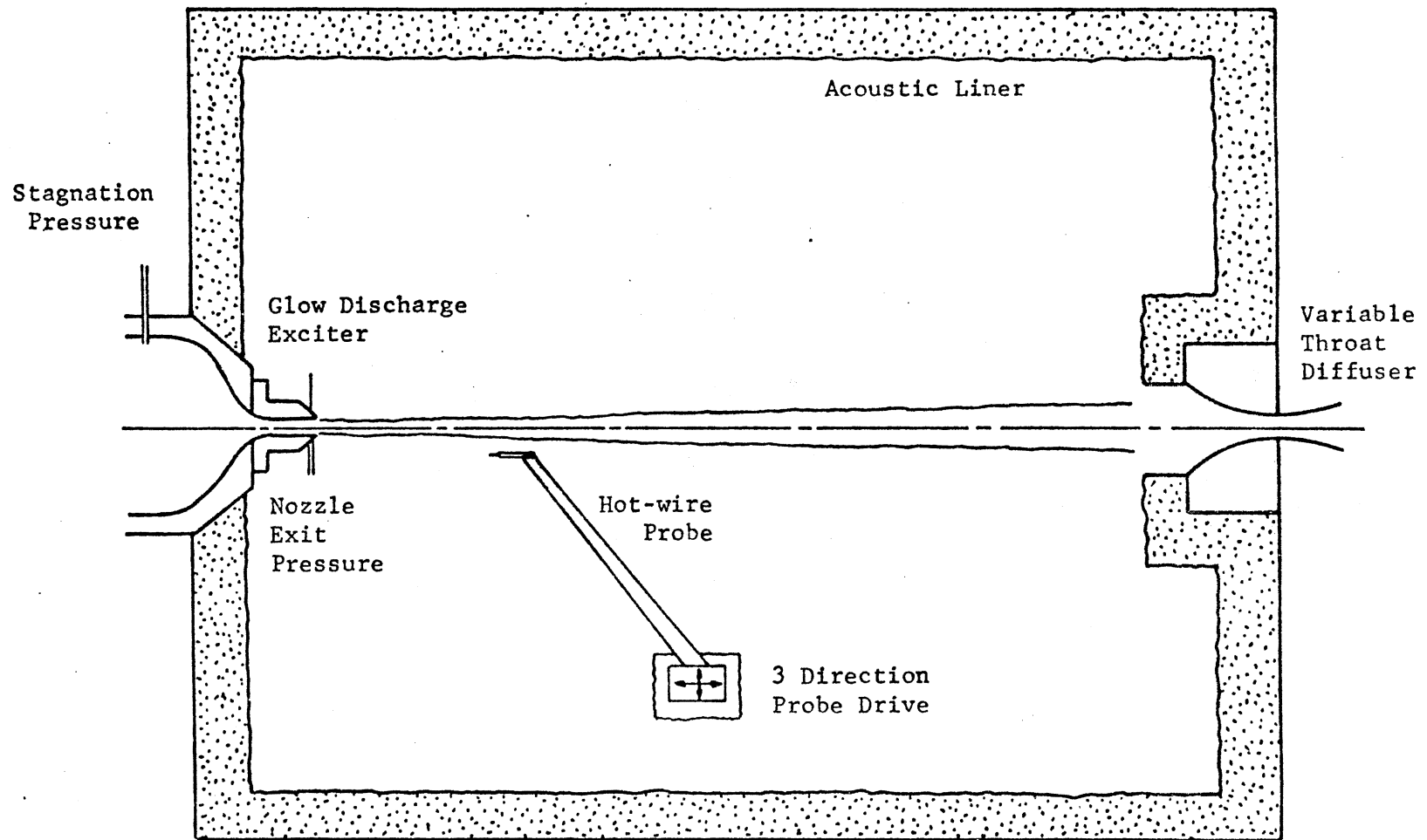


Figure 2. Schematic of Test Chamber

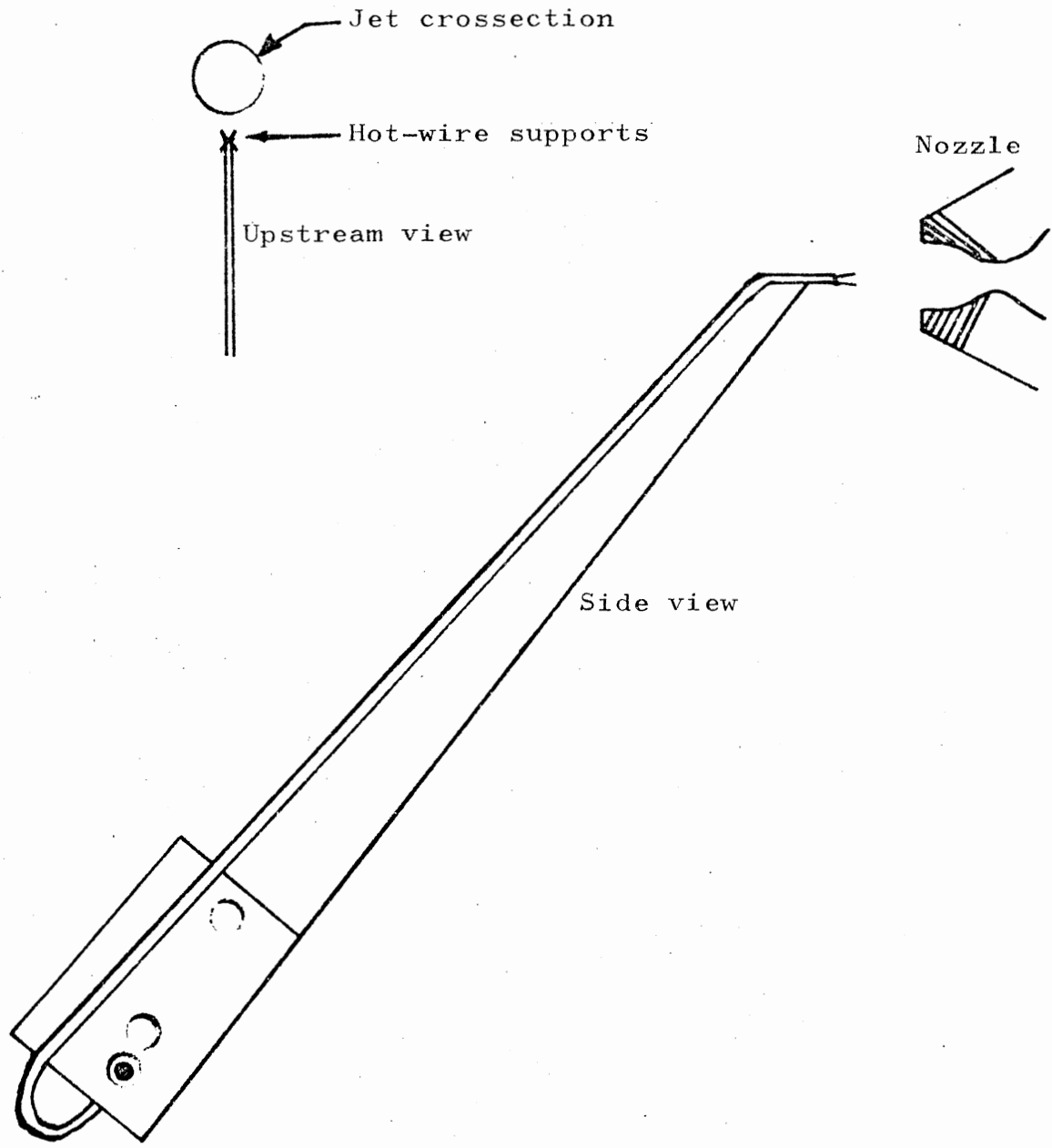


Figure 3. Crossed Hot-Wire Probe, Full Scale

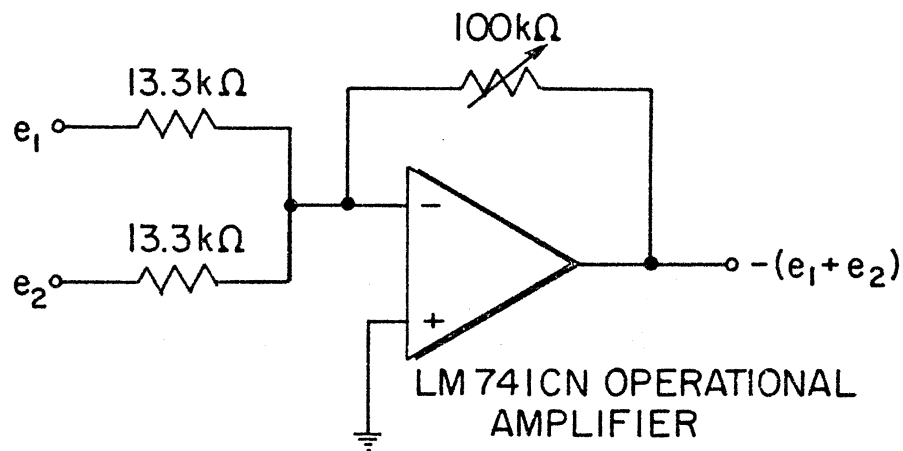
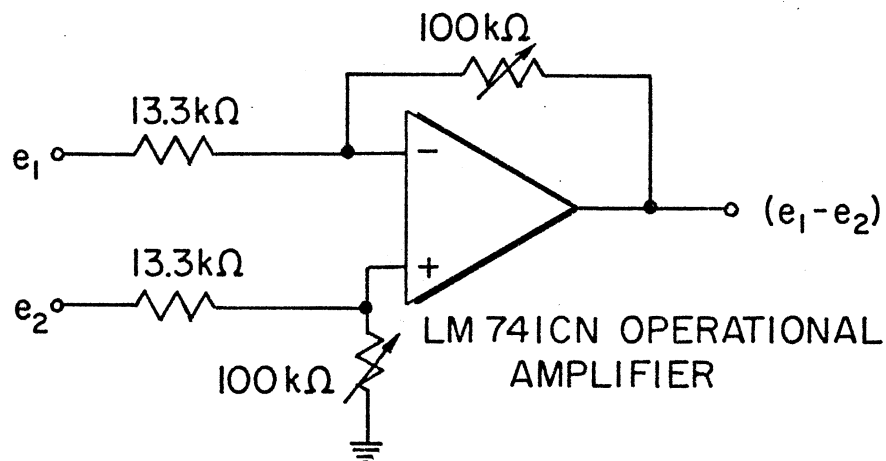
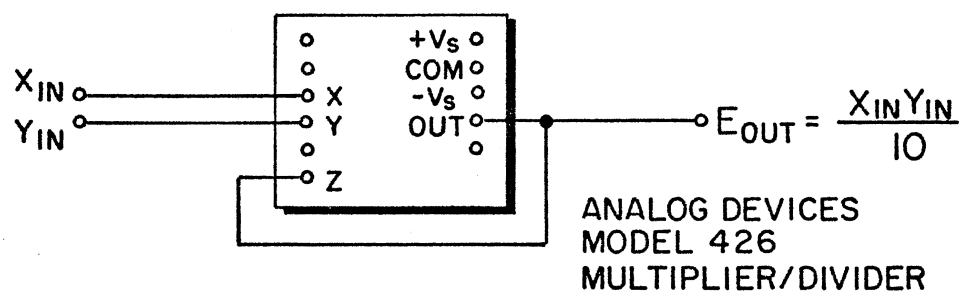
ADDER CIRCUITSUBTRACTOR CIRCUITMULTIPLIER CIRCUIT

Figure 4. Schematic of Electronic Devices

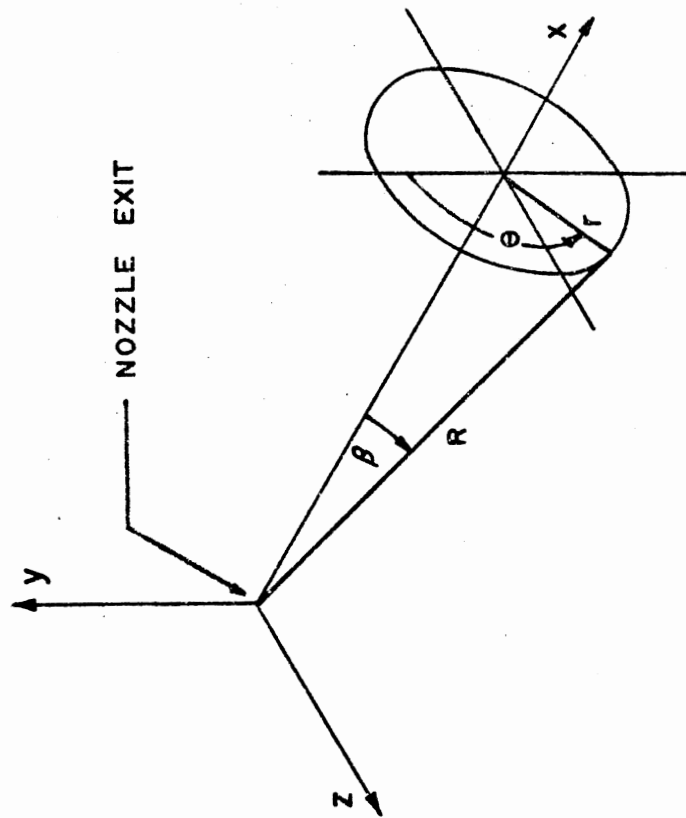
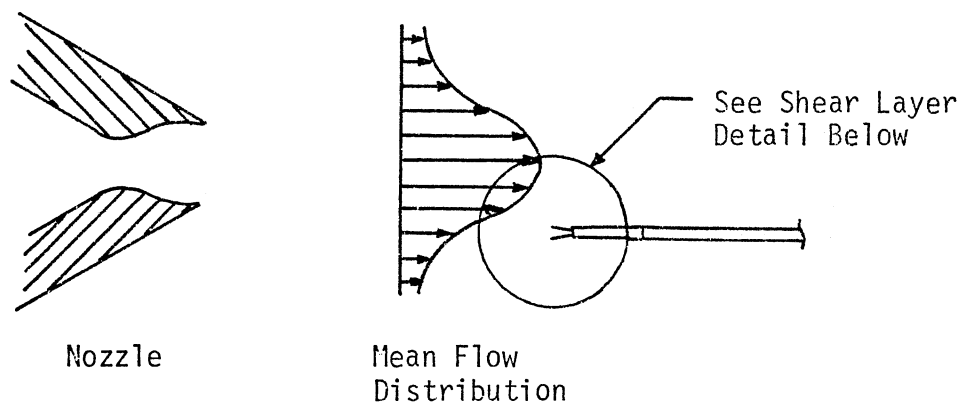


Figure 5. Facility Coordinate System



Detail

(Probes are shown in relative size to one another)

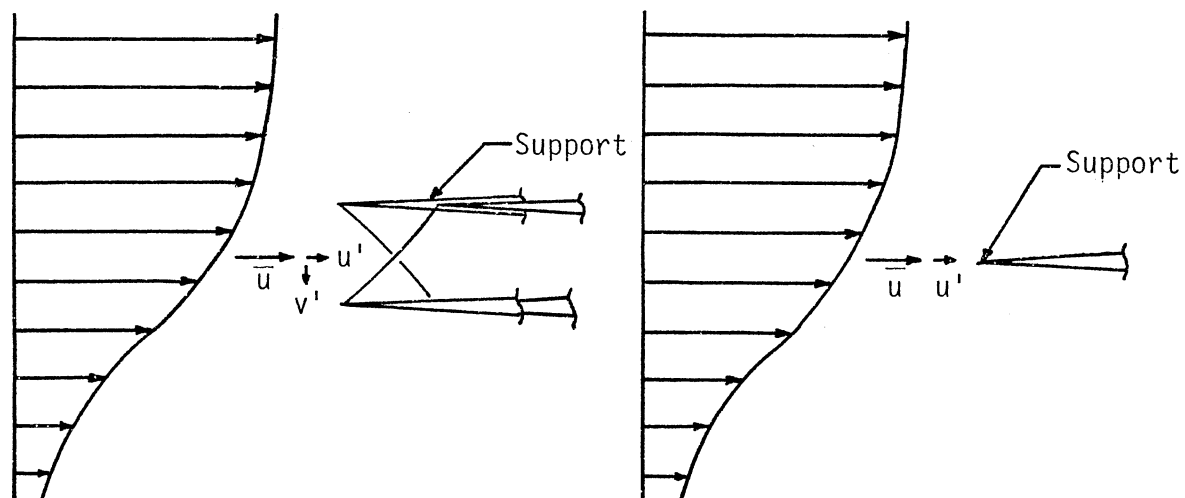


Figure 6. Schematic of Crossed Hot-Wire Probe Orientation

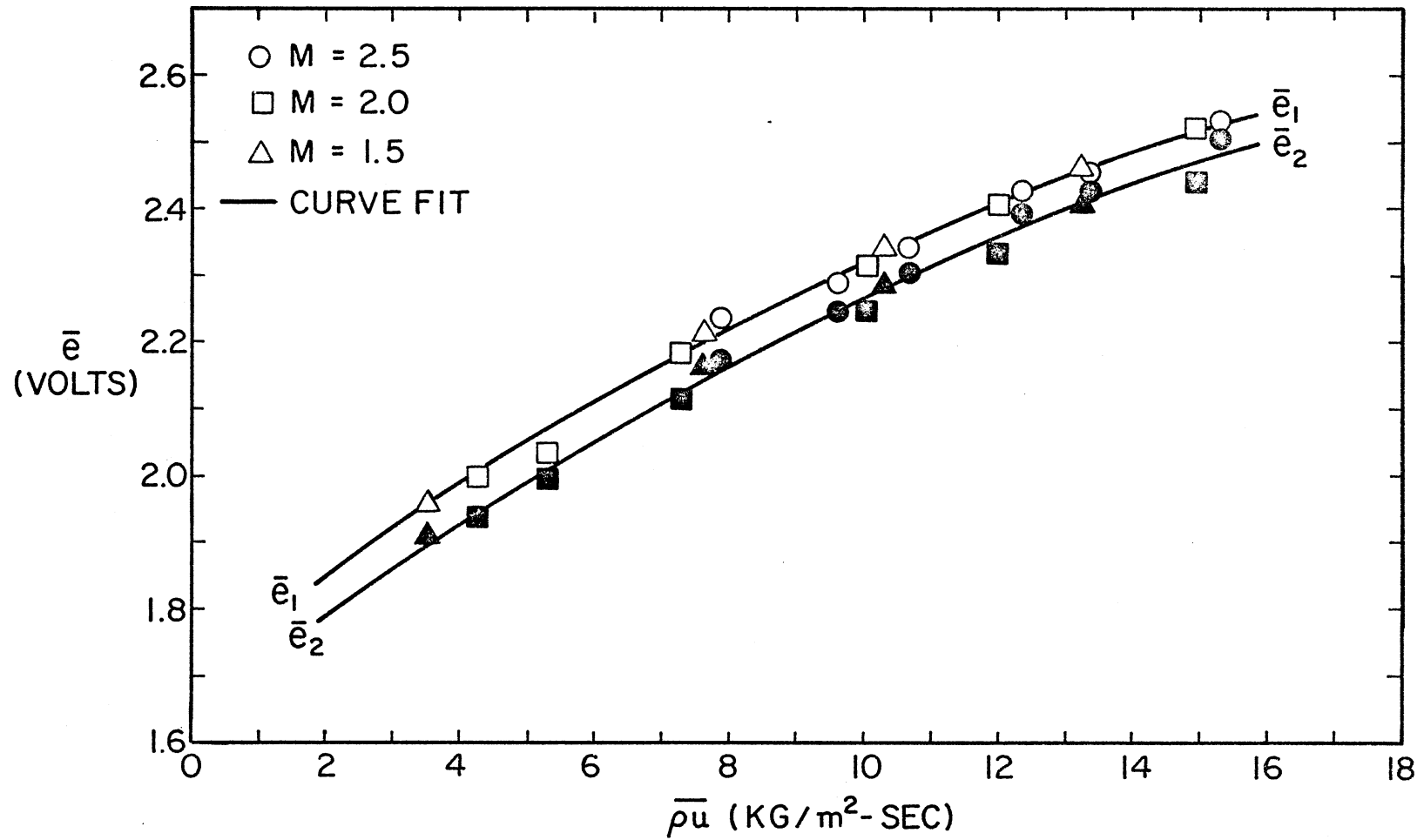


Figure 7. Crossed Hot-Wire Calibration, \bar{e} as a Function of $\bar{\rho}u$

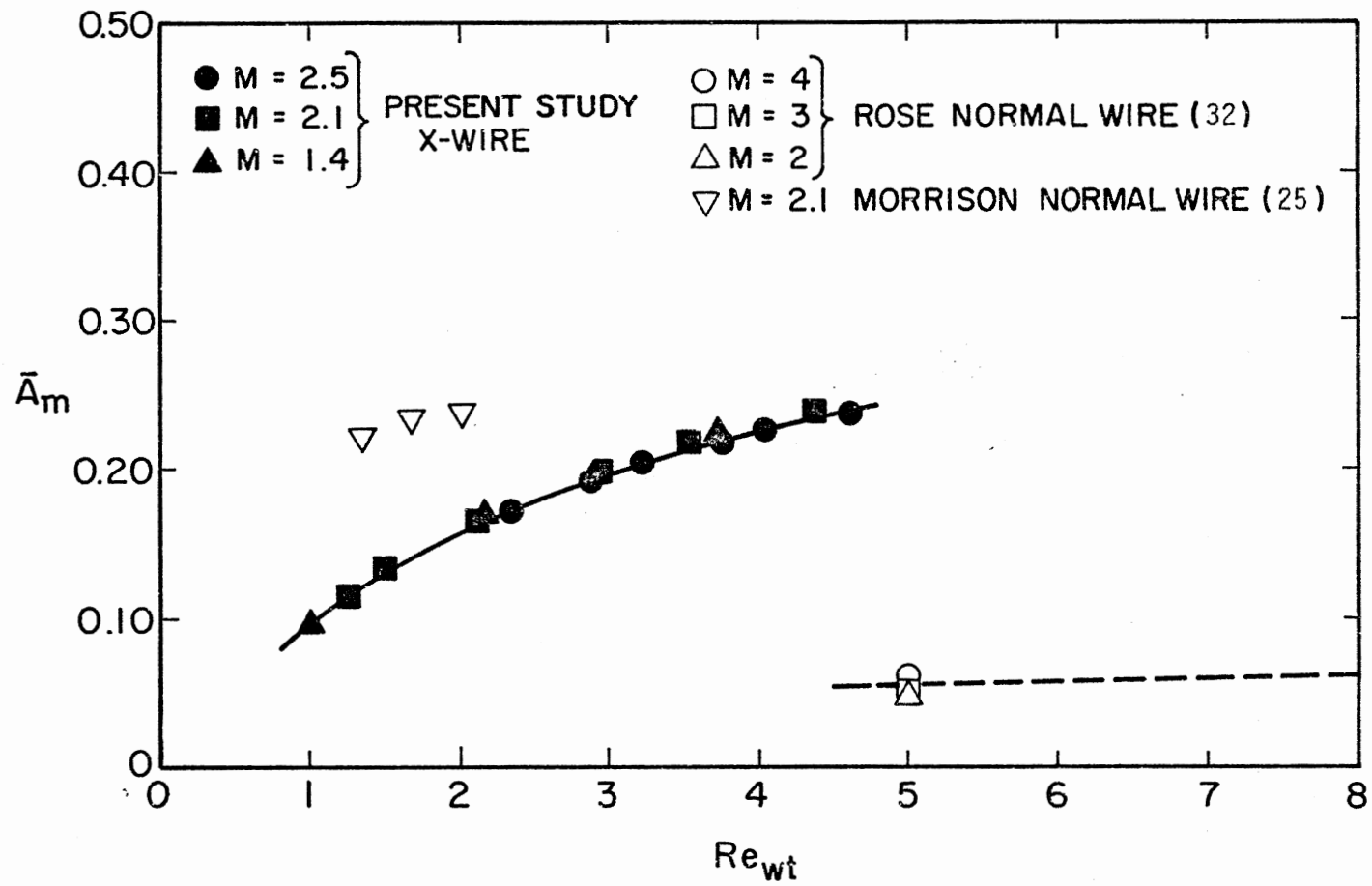


Figure 8. Crossed Hot-Wire Calibration, \bar{A}_m as a Function of Re_{wt}

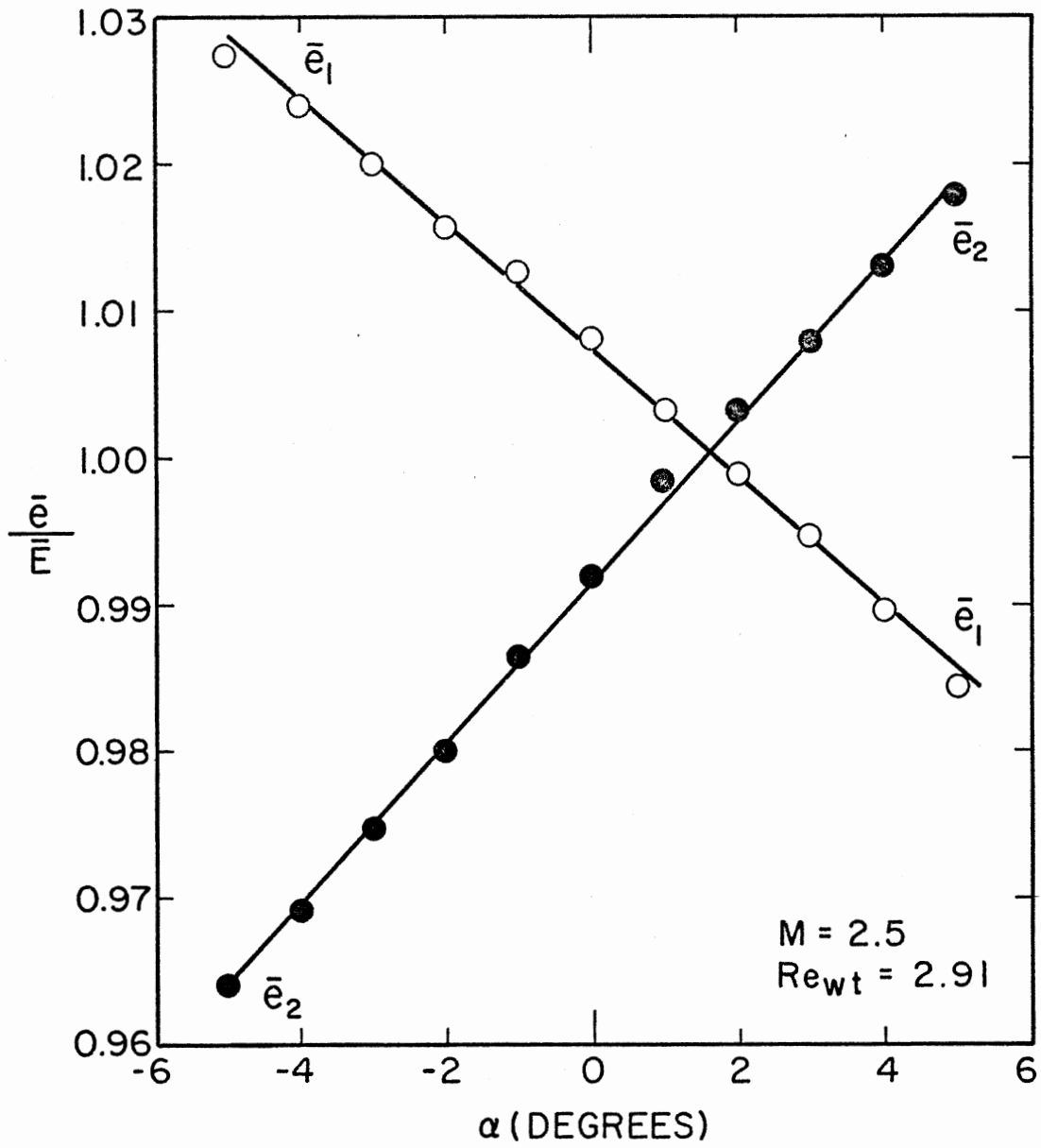


Figure 9. Crossed Hot-Wire Calibration, \bar{e}/\bar{E} as a Function of α

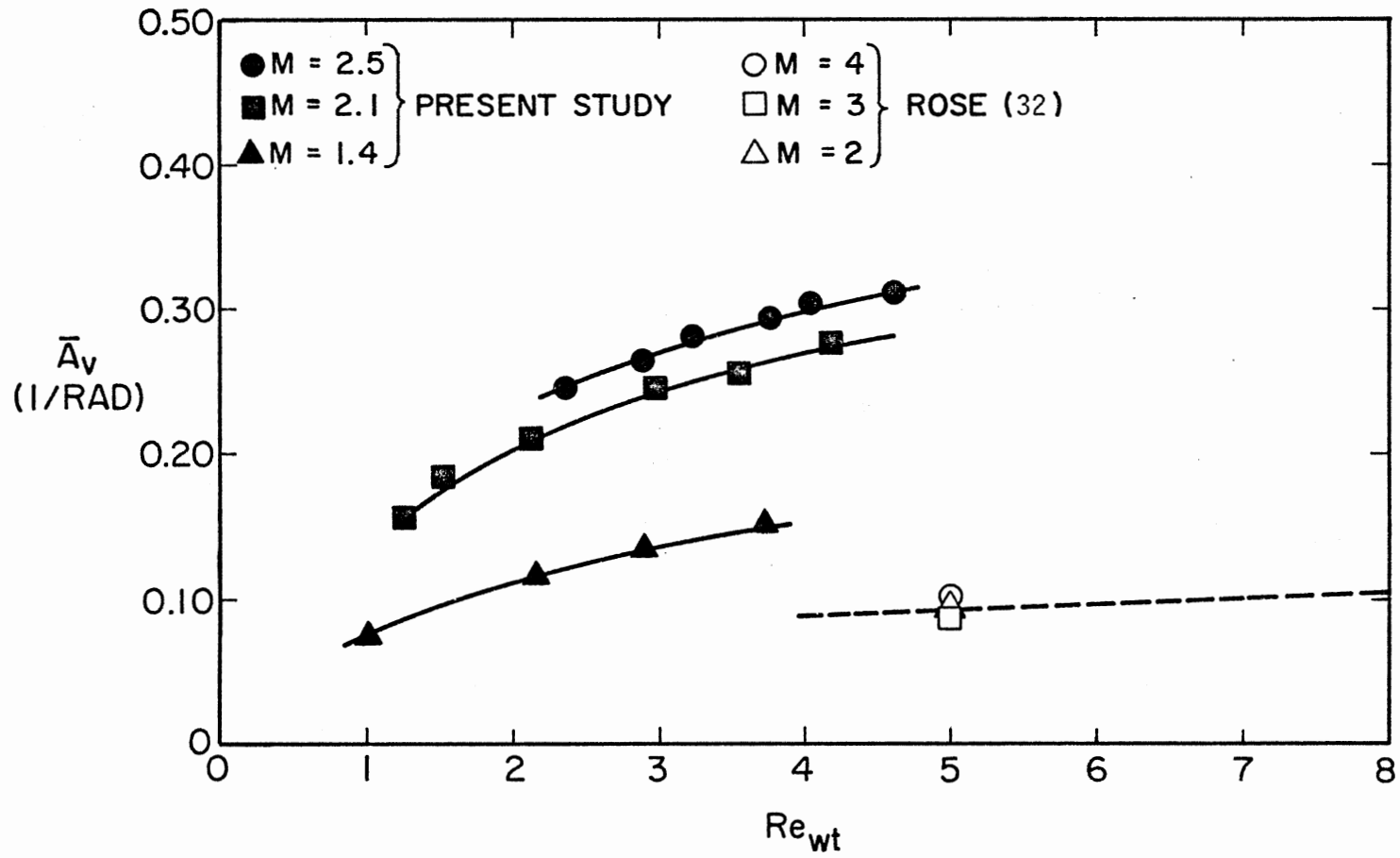


Figure 10. Crossed Hot-Wire Calibration, \bar{A}_v as a Function of Re_{wt}

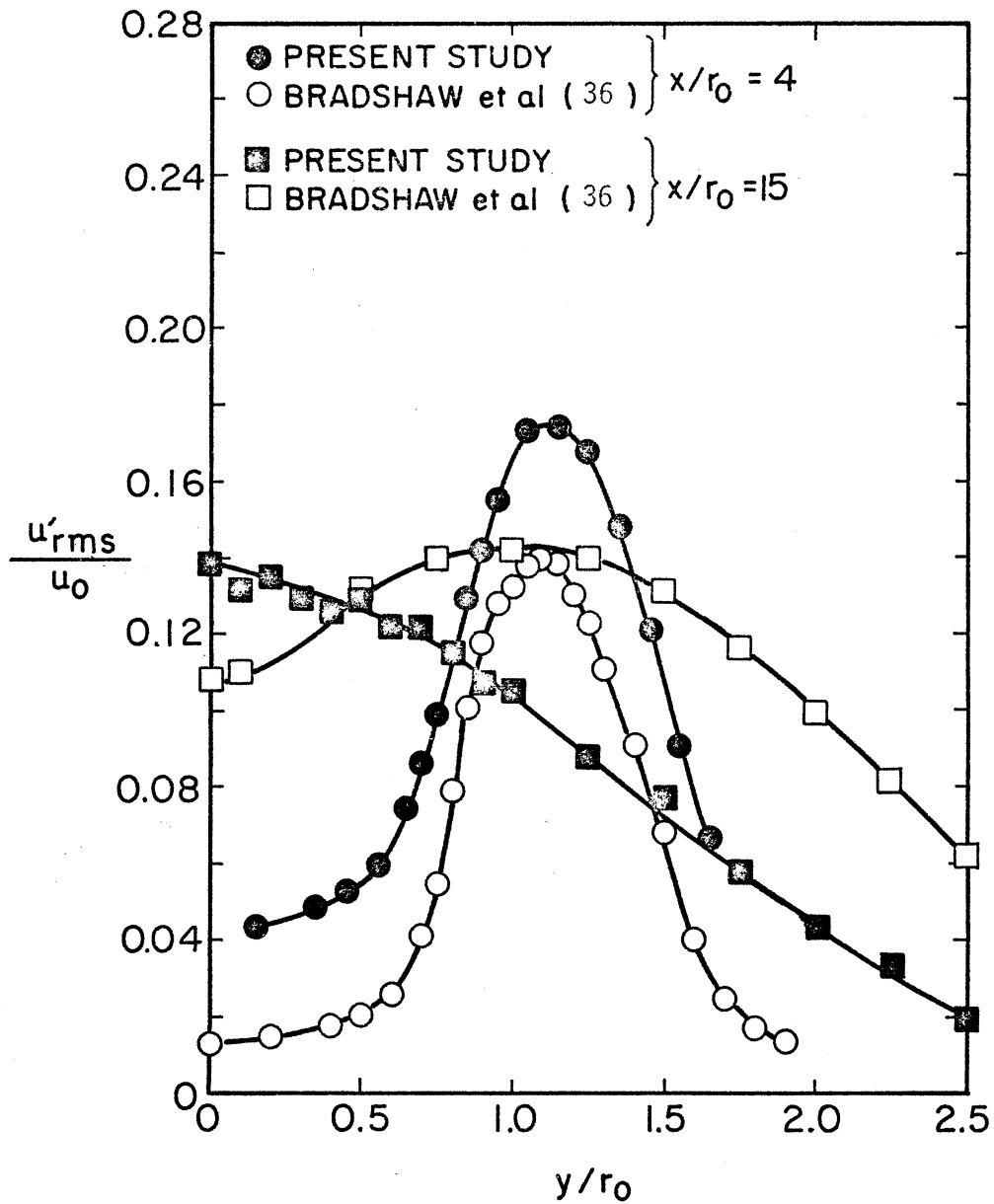


Figure 11. Radial Profiles of Axial Velocity Turbulence Intensity for the Subsonic Jet

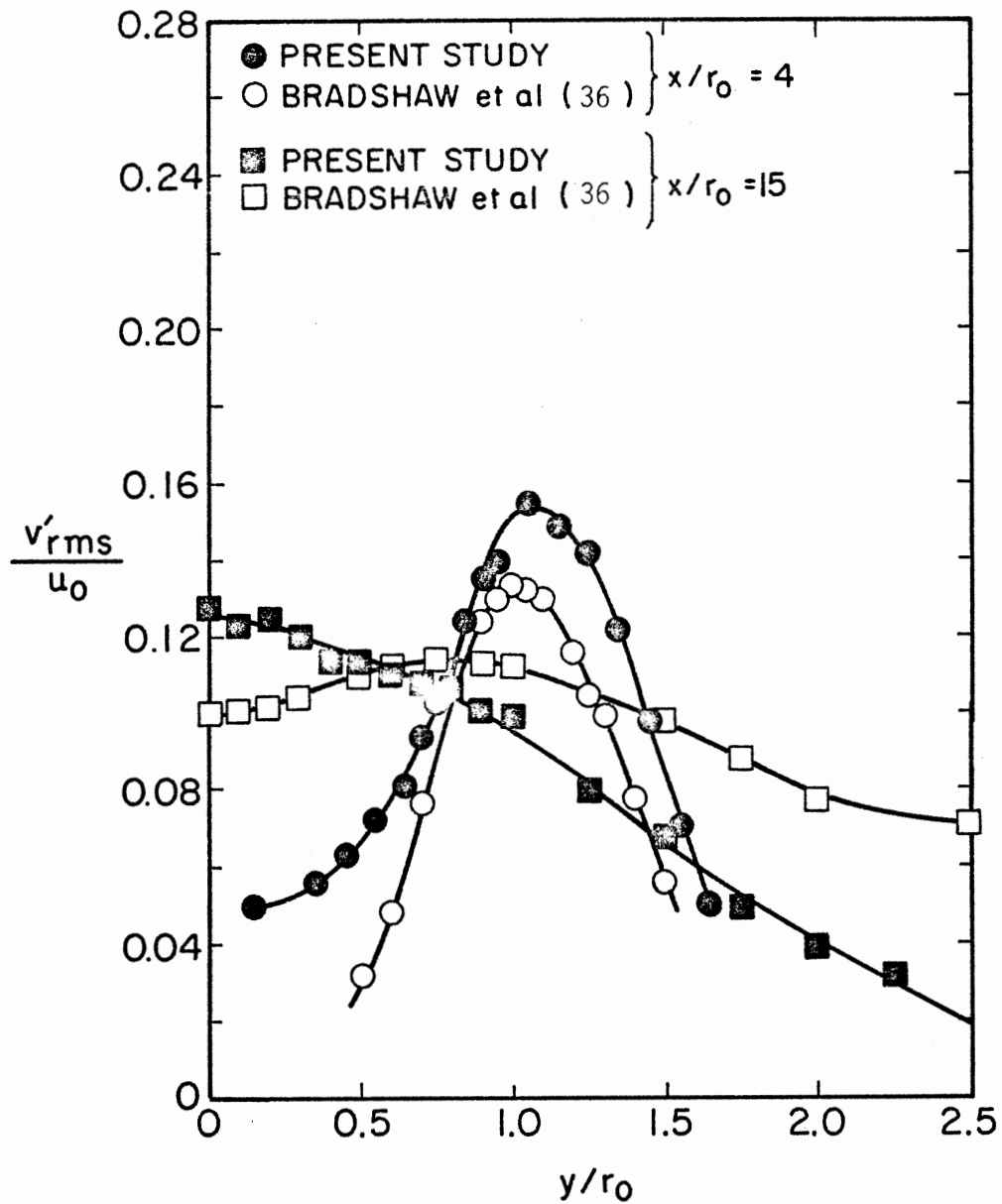


Figure 12. Radial Profiles of Radial Velocity Turbulence Intensity for the Subsonic Jet

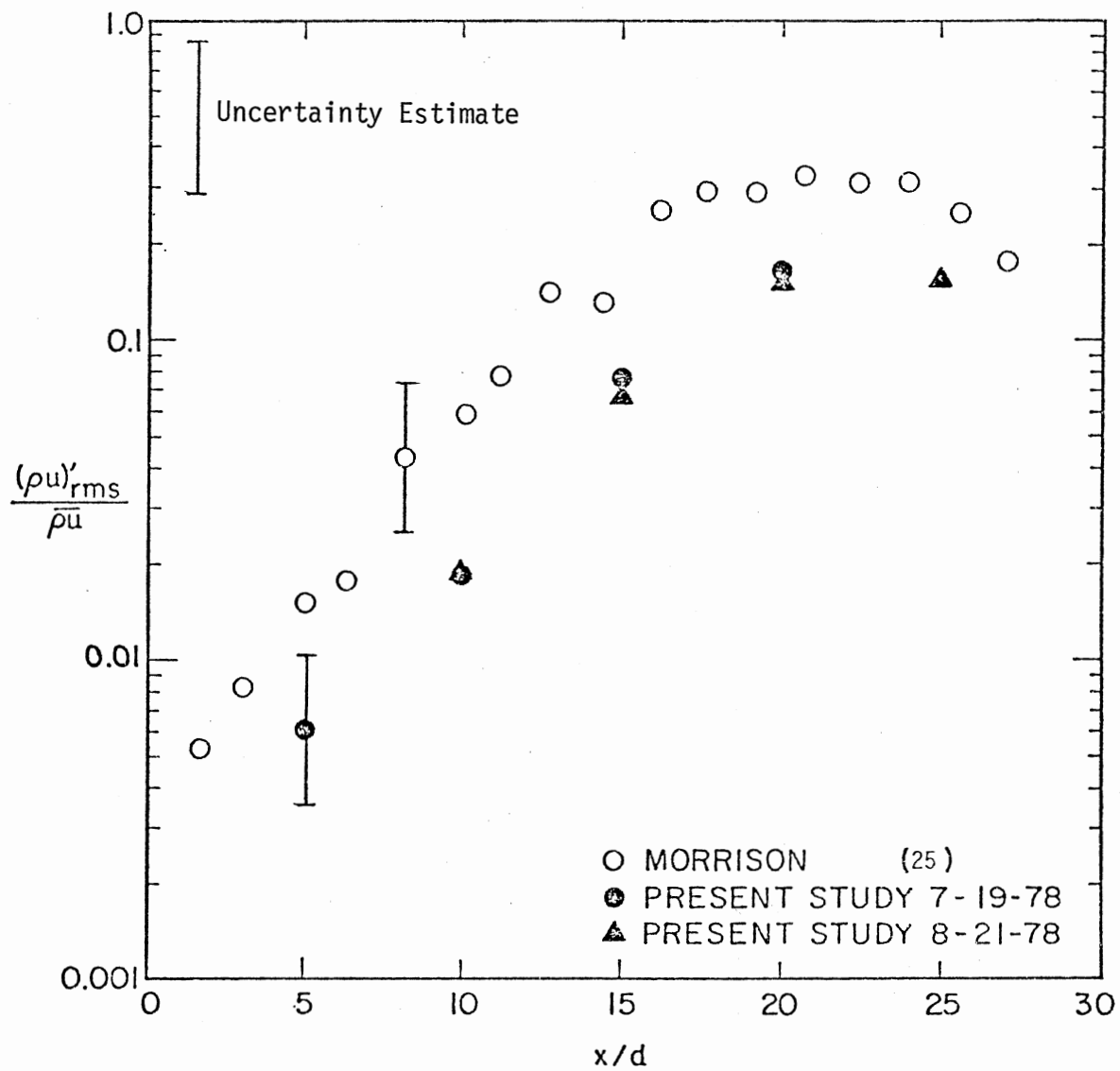


Figure 13. Axial Distribution of Peak Mass Velocity Fluctuations, $M = 2.5$

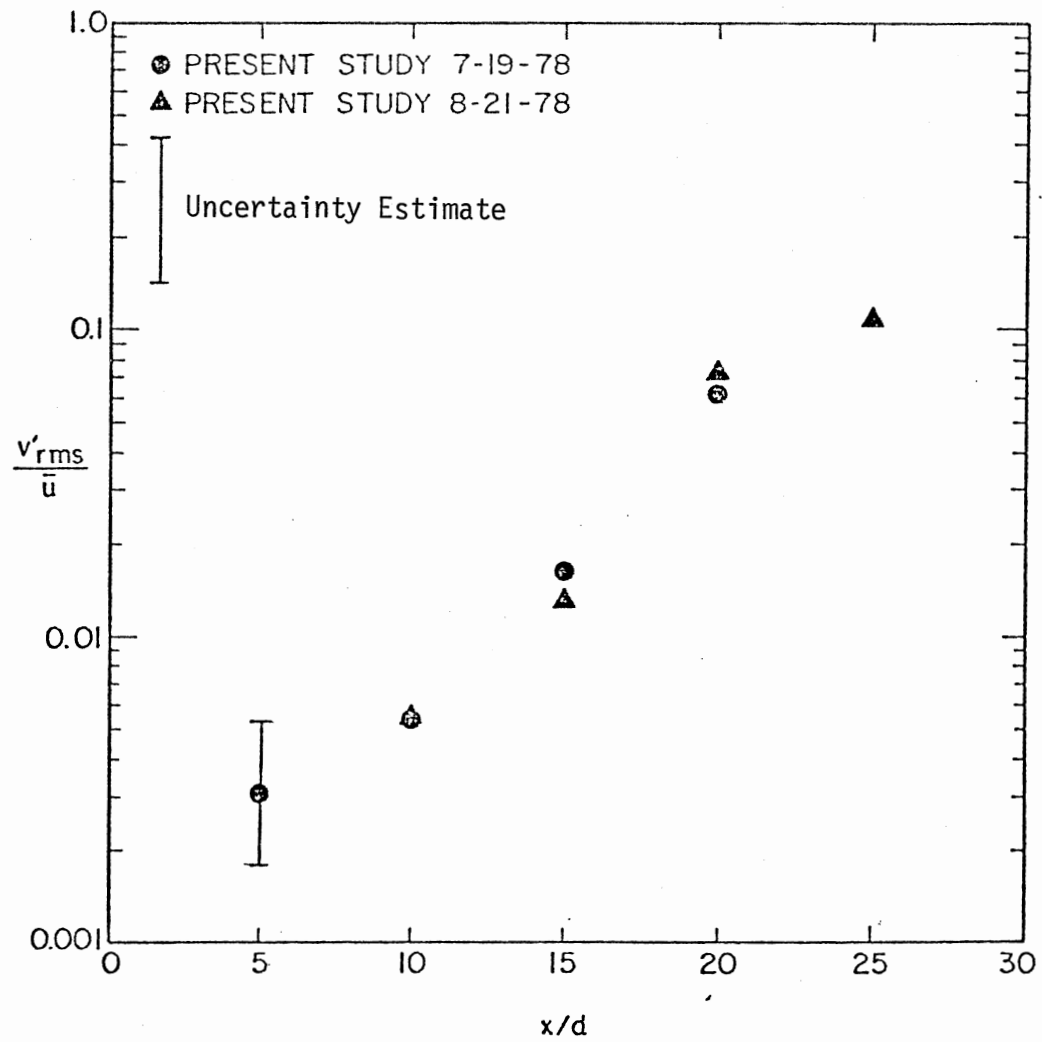


Figure 14. Axial Distribution of Peak Radial Velocity Fluctuations, $M = 2.5$

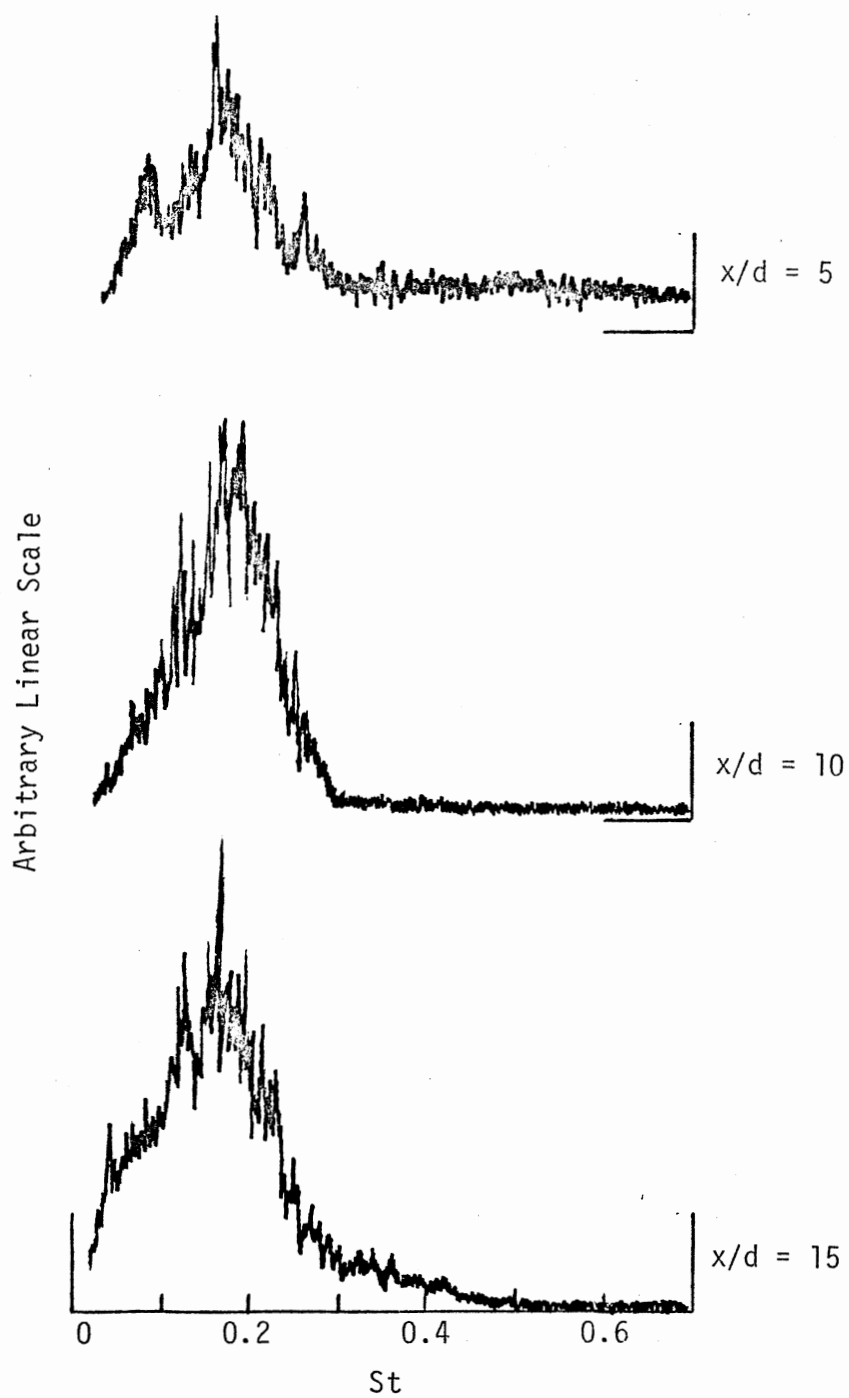


Figure 15. Crossed Hot-Wire Mass Velocity Spectra in the Jet Shear Layer, $M = 2.5$

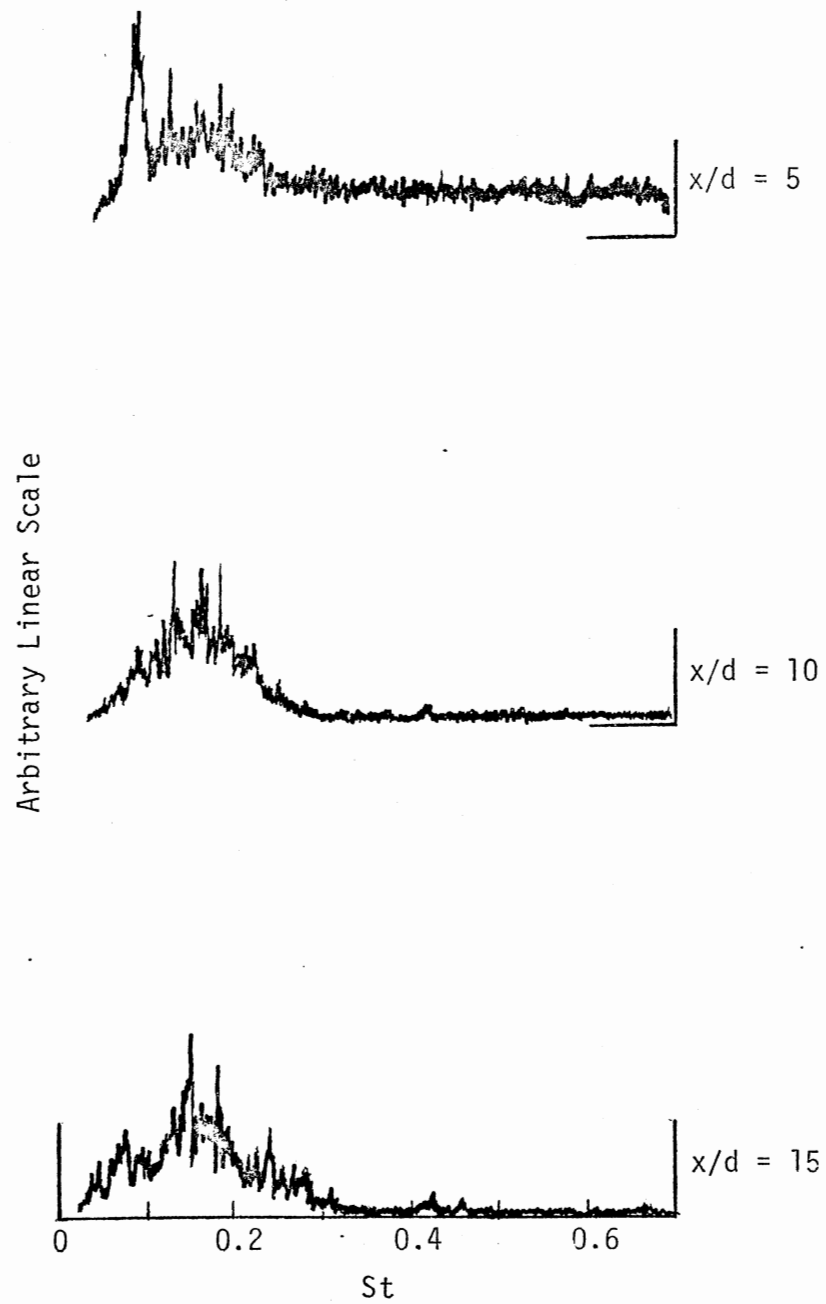


Figure 16. Crossed Hot-Wire Radial Velocity Spectra in the Jet Shear Layer, $M = 2.5$

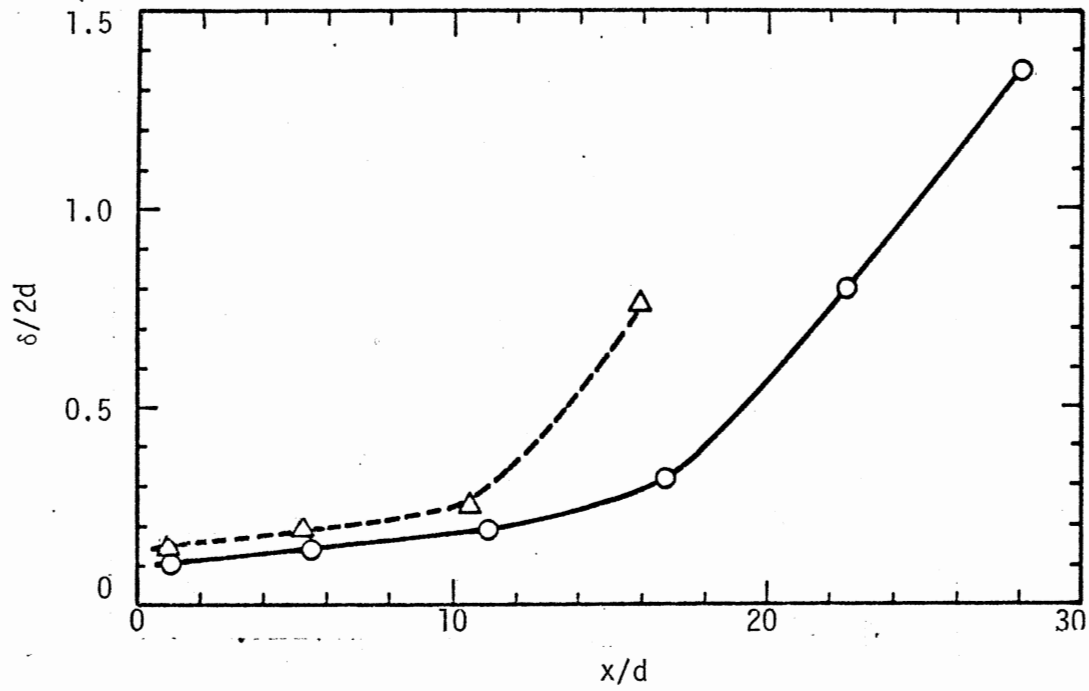
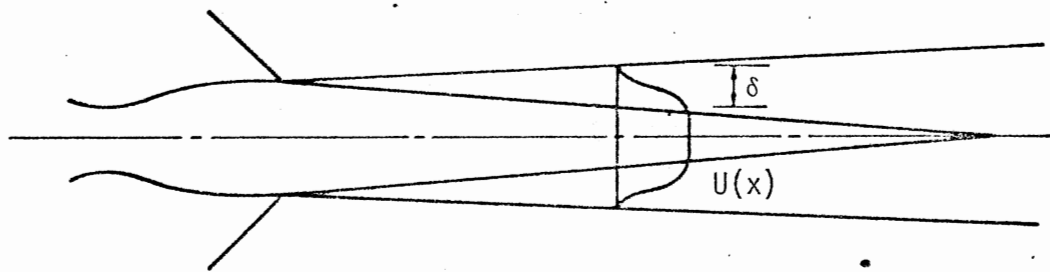


Figure 17. Variation of Shear Layer Half-Thickness Parameter ($\delta/2d$) With Downstream Distance
 $\Delta M = 2.1$, $OM = 2.5$

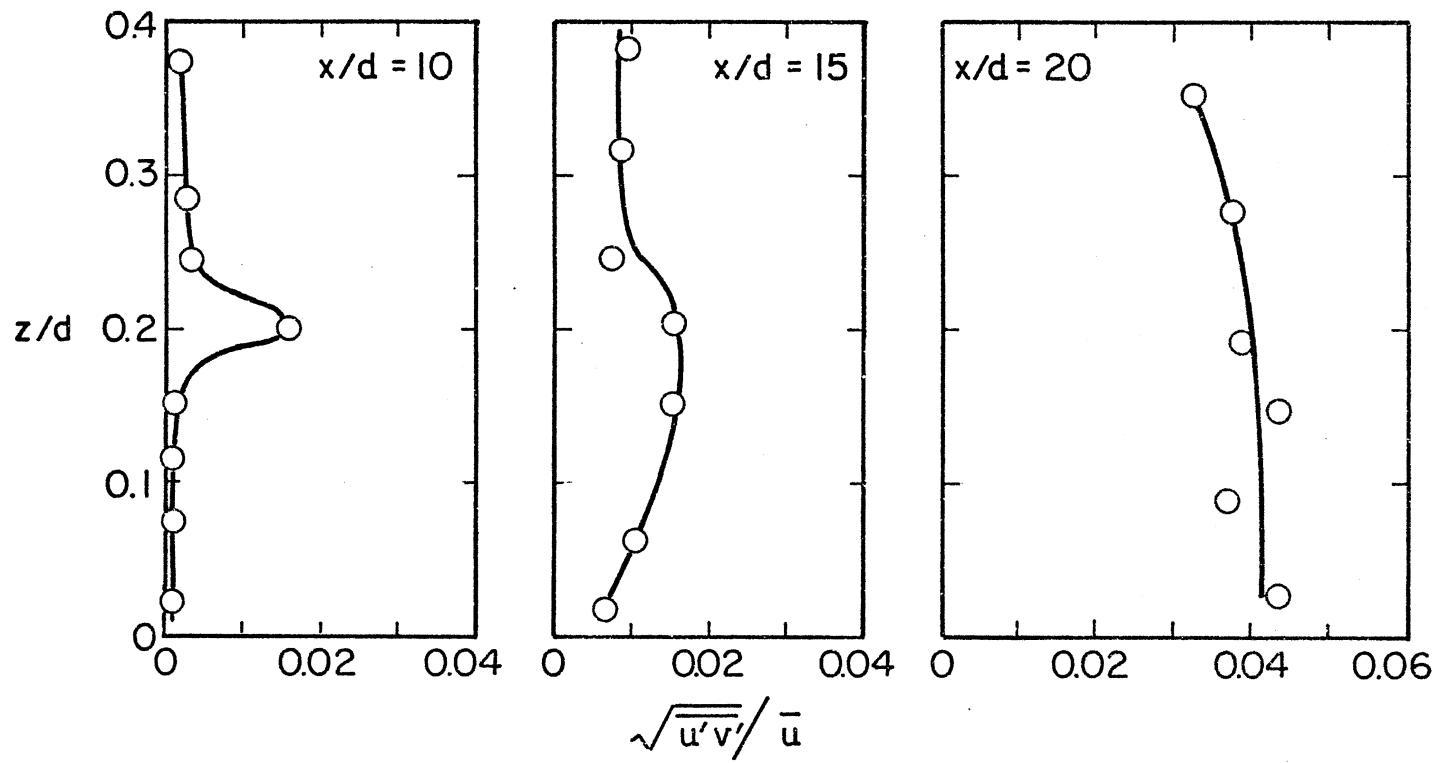


Figure 18. Radial Distributions of Velocity Covariance, $\sqrt{\overline{u'v'}}/\bar{u}$, $M = 2.5$

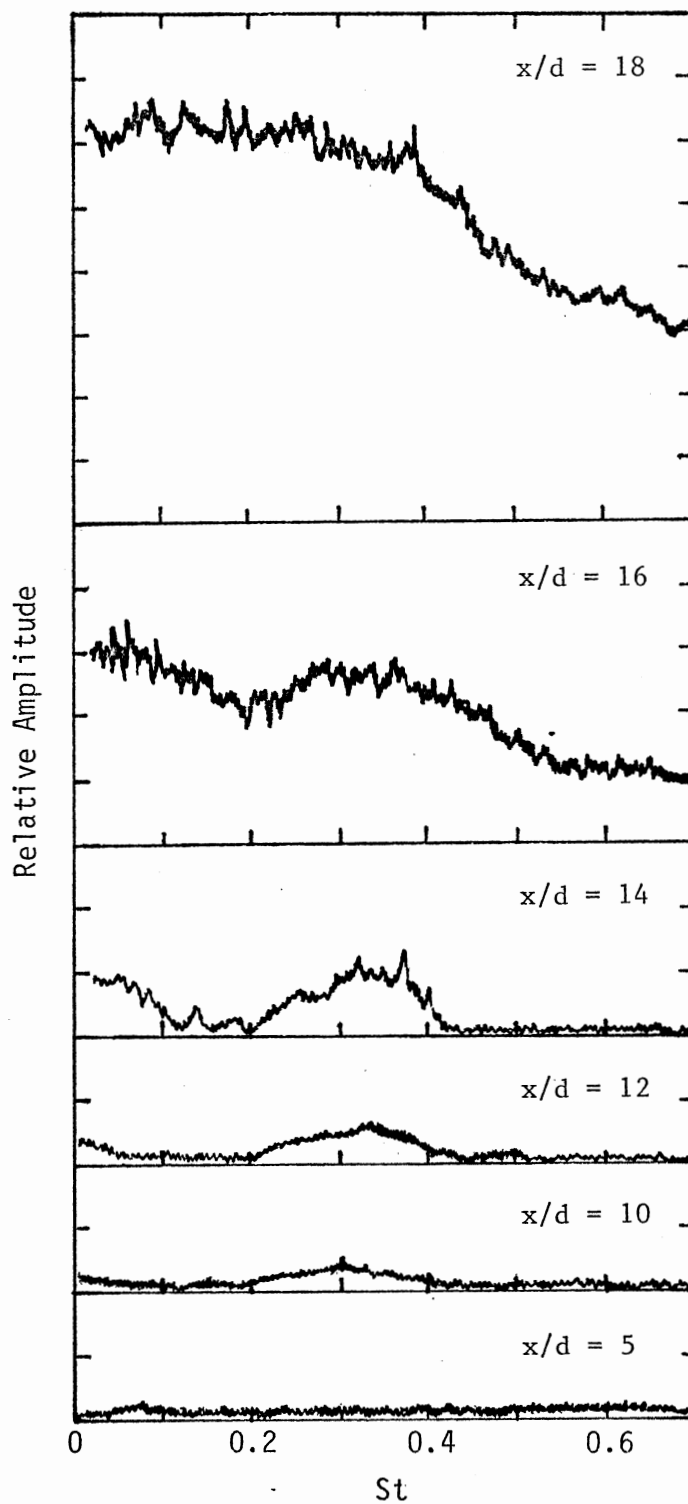


Figure 19. Momentum Transport, $(\rho u)'v'$, Spectra in the Jet Shear Layer, Unexcited $M = 2.5$

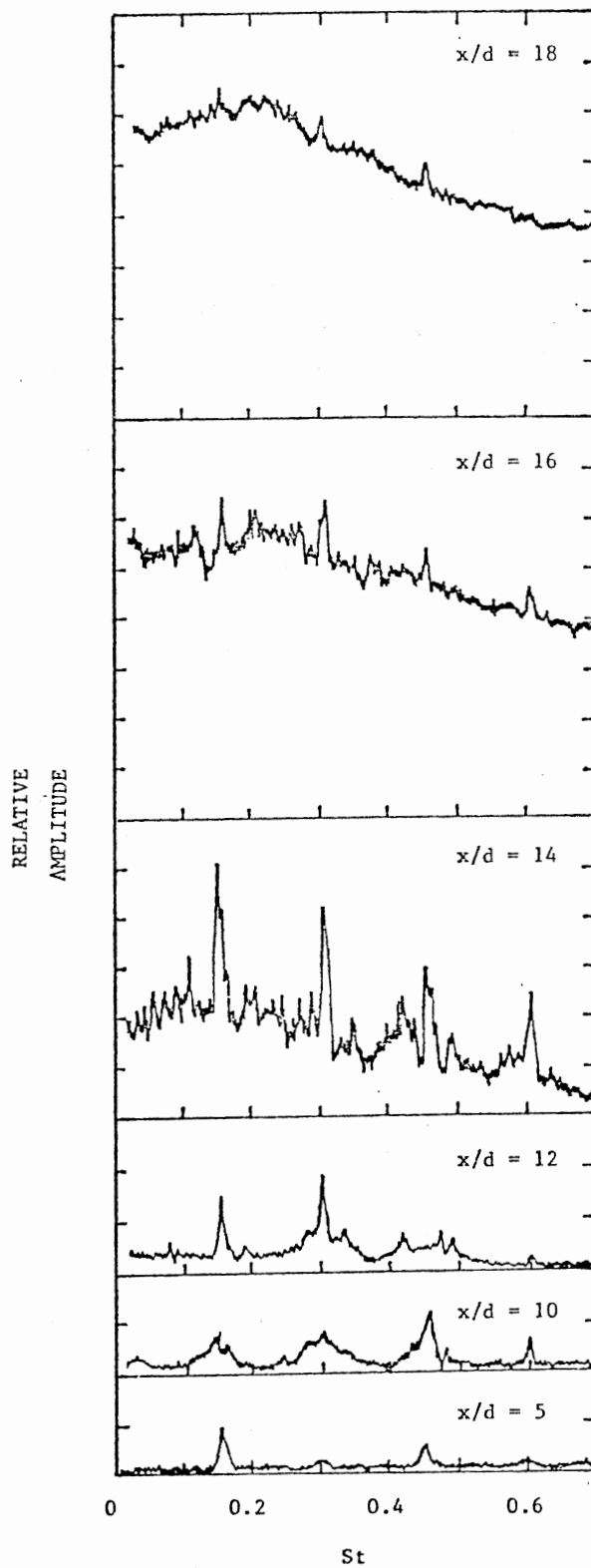


Figure 20. Momentum Transport, $(\rho u)'v'$, Spectra in the Jet Shear Layer, Excited $M = 2.5$

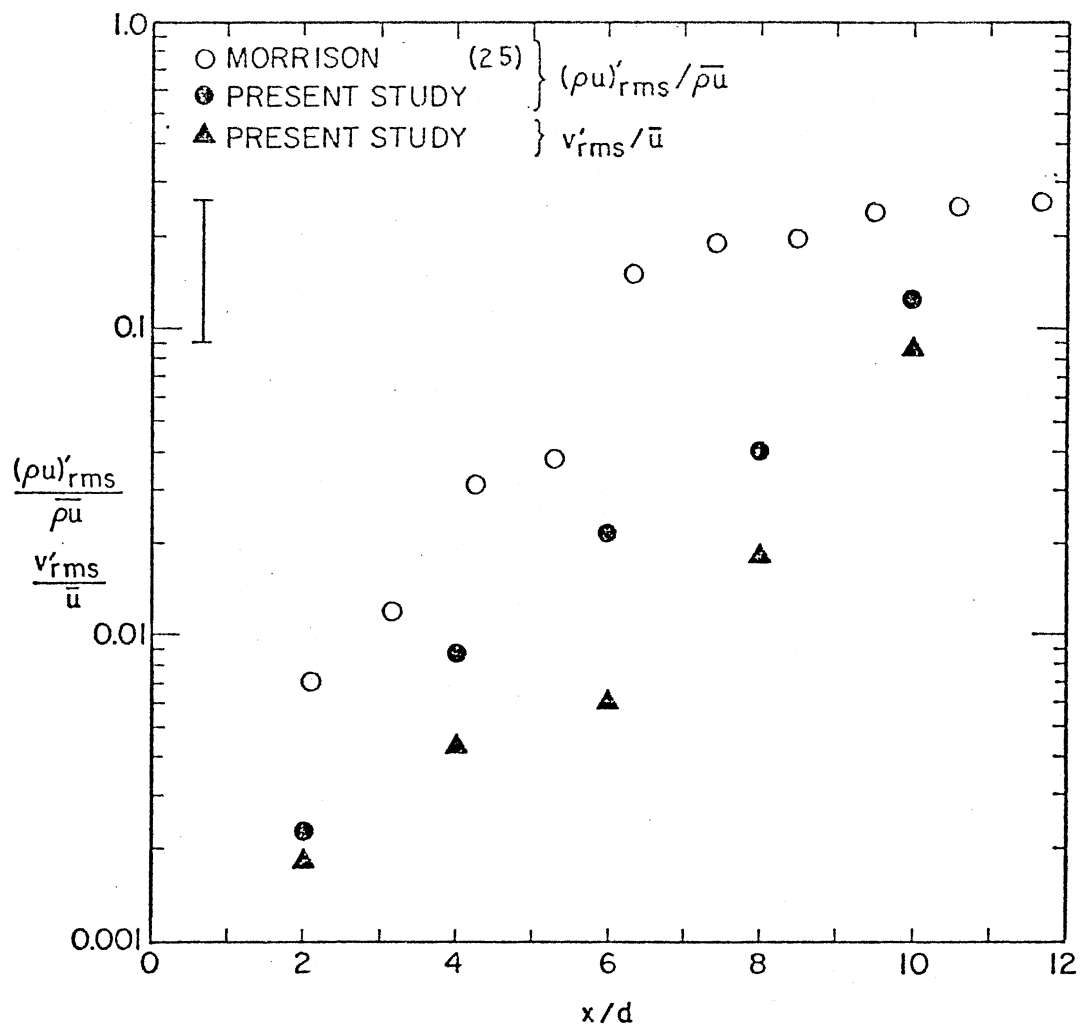


Figure 21. Axial Distributions of Peak Mass Velocity and Peak Radial Velocity Fluctuations, $M = 2.1$

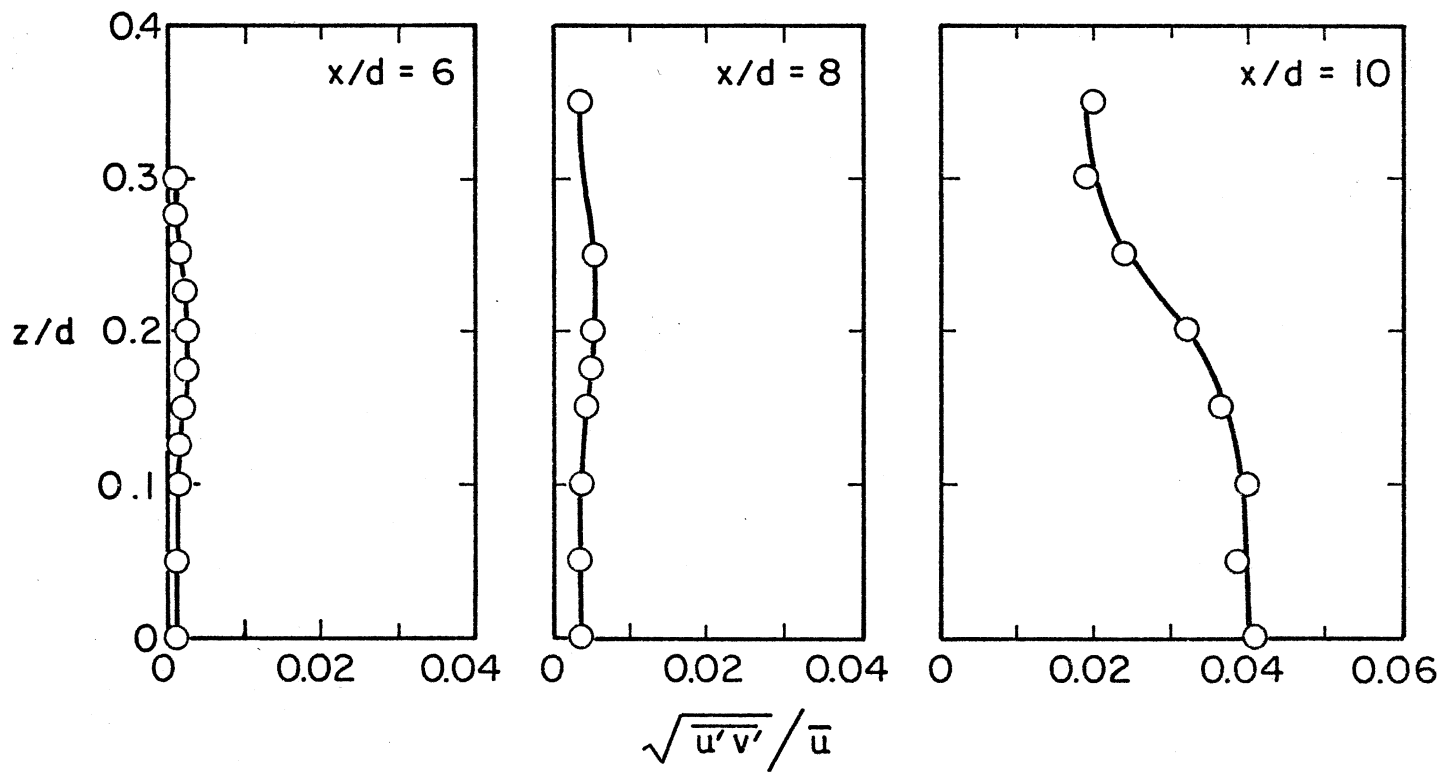


Figure 22. Radial Distributions of Velocity Covariance, $\sqrt{u'v'}/\bar{u}$, $M = 2.1$

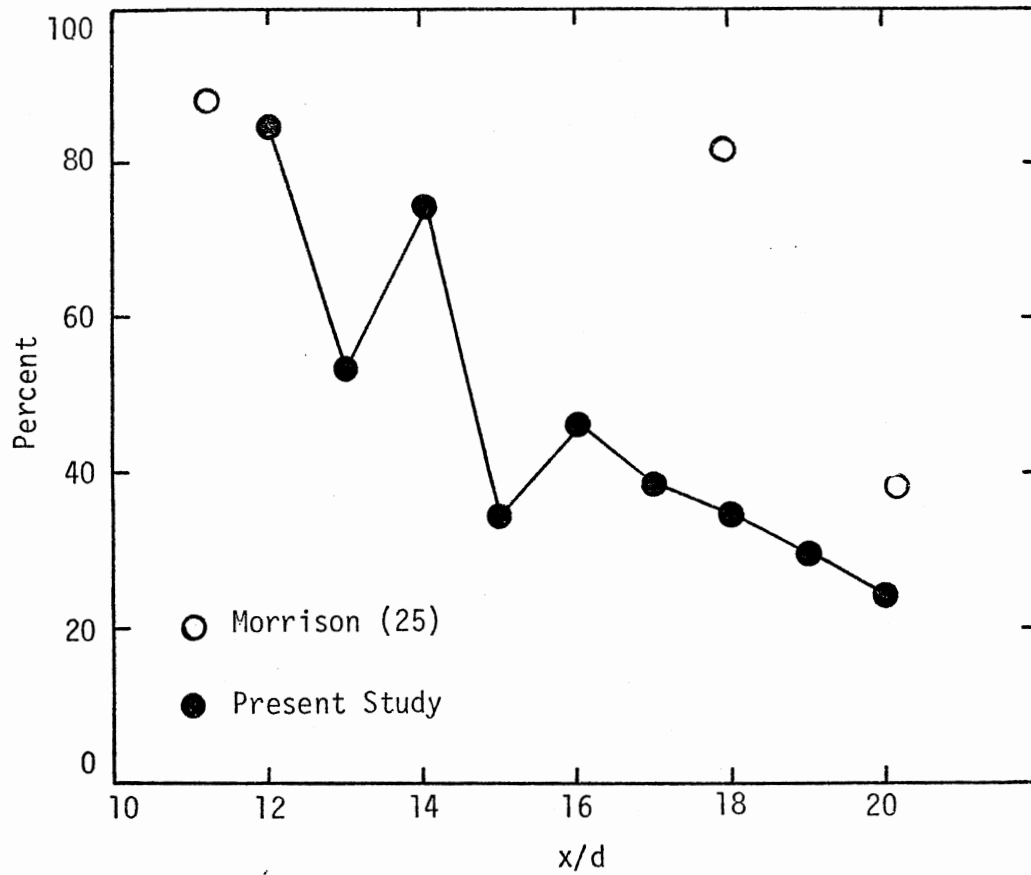


Figure 23. Axial Distribution of Percent Coherent Structure, $\langle(\rho u)'\rangle_{rms}/(\rho u)'\rangle_{rms}$, in the Mass Velocity Fluctuations, $M = 2.5$

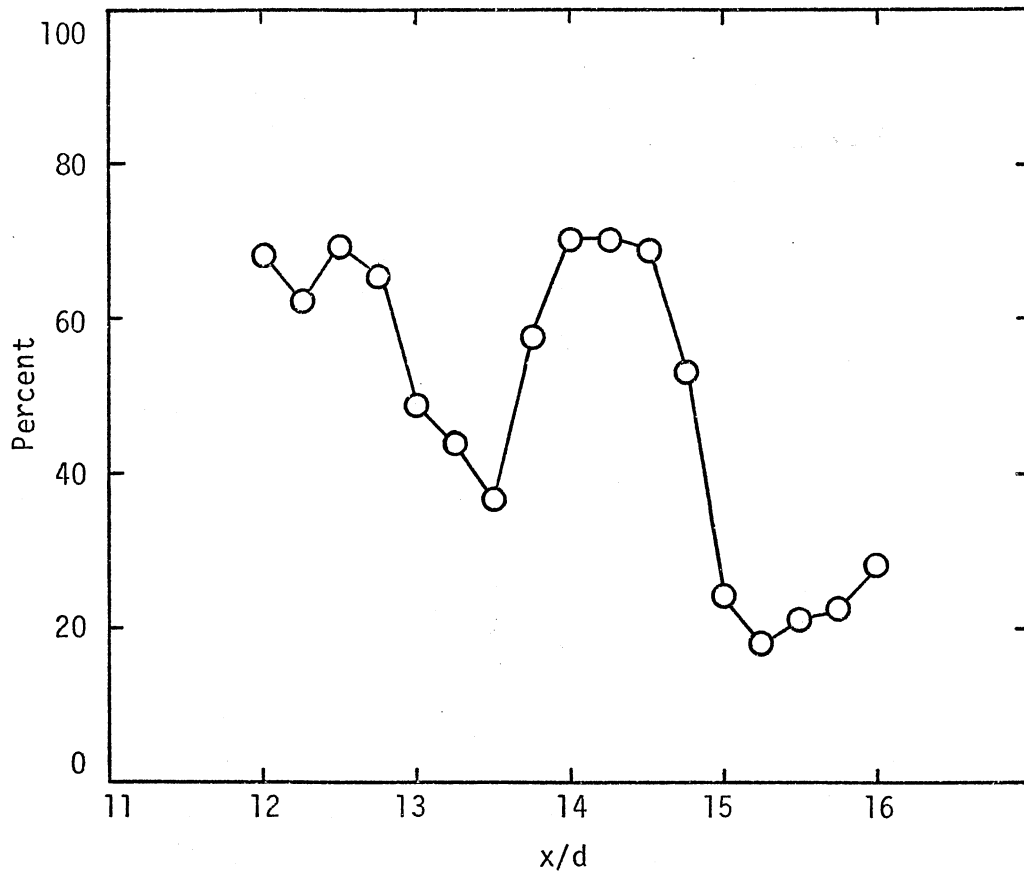


Figure 24. Wavelength Measurement of Axial Coherent Structure Oscillation, $M = 2.5$

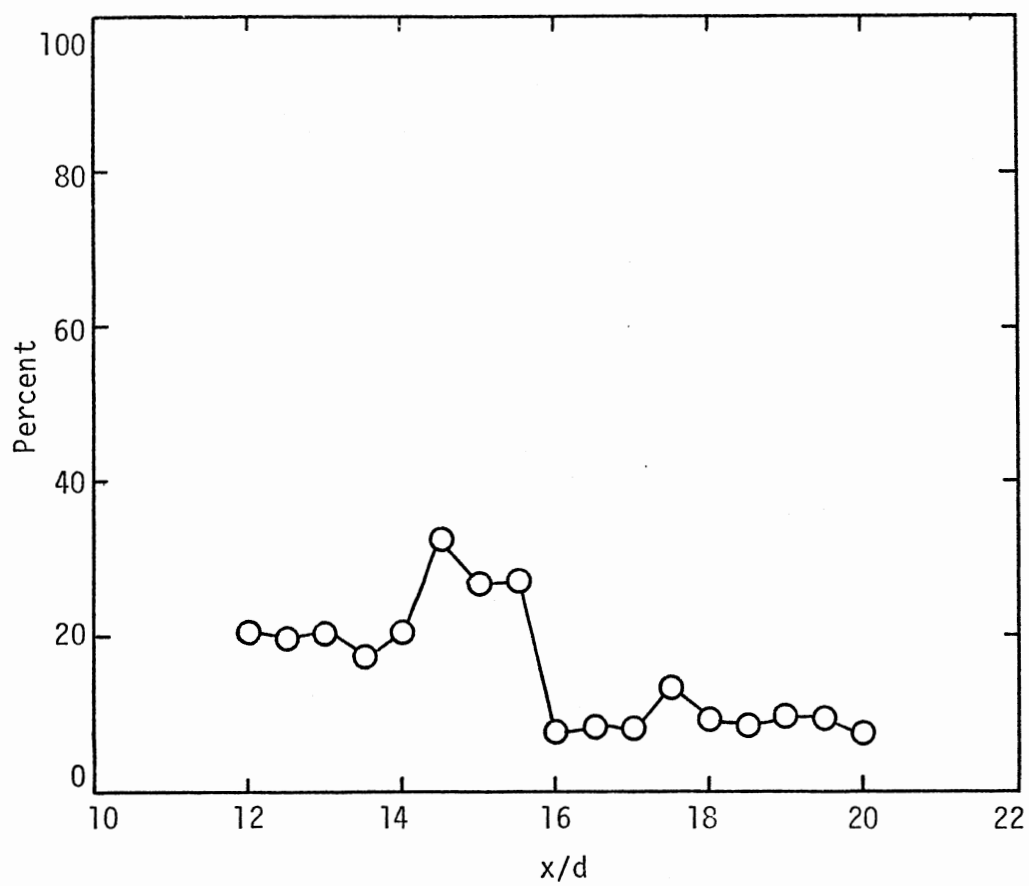


Figure 25. Axial Distribution of Percent Coherent Structure, $\langle(\rho u)'v'\rangle_{\text{rms}}/[(\rho u)'v']_{\text{rms}}$, in the Velocity Covariance, $M = 2.5$

VITA

Jerry Dale Swearingen

Candidate for the Degree of
Master of Science

Thesis: **CROSSED HOT-WIRE MEASUREMENTS IN LOW REYNOLDS NUMBER SUPERSONIC
JETS**

Major Field: Mechanical Engineering

Biographical:

Personal Data: Born in Duncan, Oklahoma, July 29, 1955, the son of
Mr. and Mrs. Dale D. Swearingen.

Education: Graduated from Bishop McGuinness High School in
Oklahoma City, Oklahoma, in May, 1973; received the Bachelor
of Science in Mechanical Engineering degree from Oklahoma
State University, Stillwater, Oklahoma, in December, 1977;
completed requirements for the Master of Science degree at
Oklahoma State University in December, 1979.

Honors: American Petroleum Institute Scholarship, Texaco Scholar-
ship, Continental Oil Company Scholarship, Tau Beta Pi, Pi Tau
Sigma.

Professional Societies: American Institute of Aeronautics and
Astronautics, American Society of Mechanical Engineers.